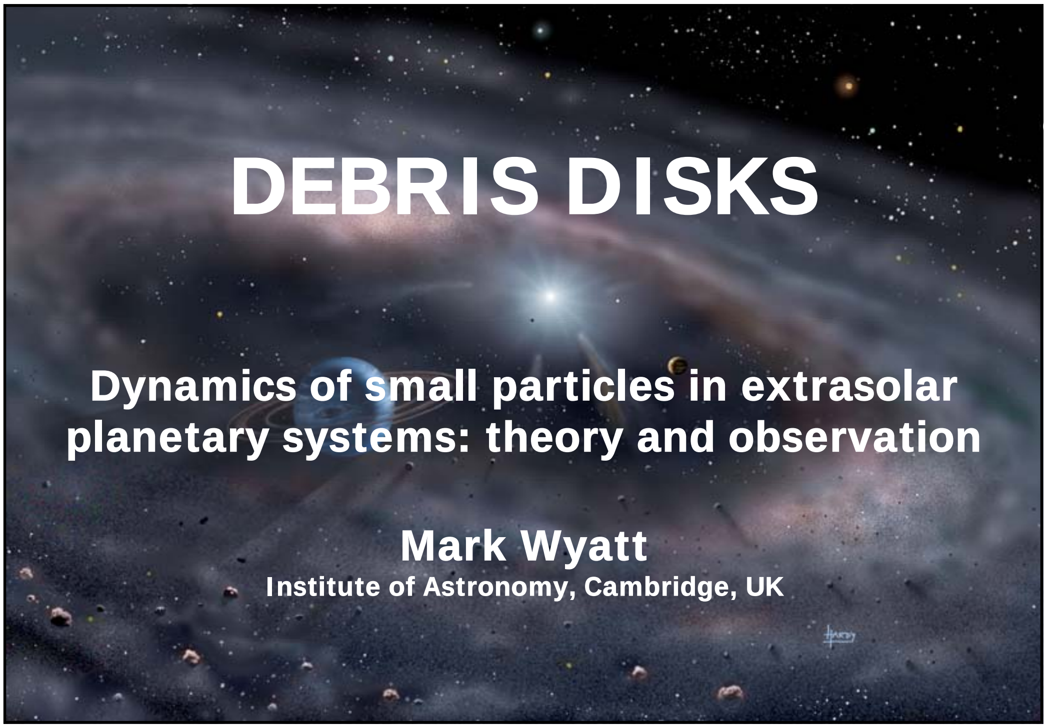

DEBRIS DISKS
Dynamics of small particles in extrasolar planetary systems: theory and observation
Mark Wyatt
Institute of Astronomy, Cambridge, UK

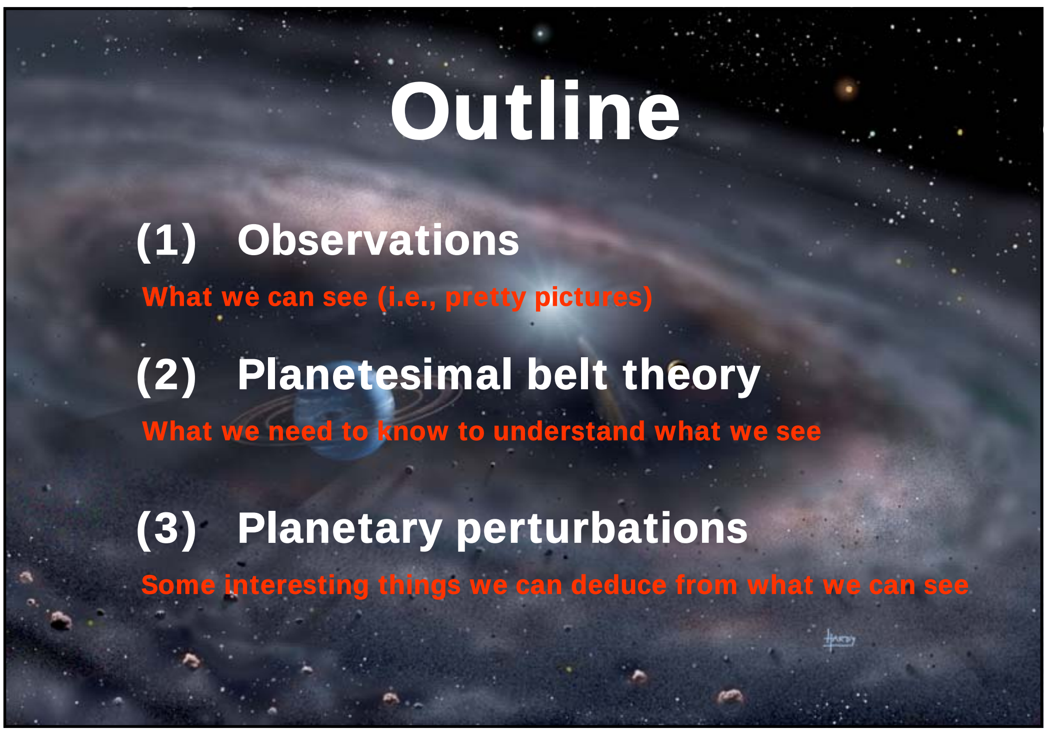

Outline
(1) Observations
What we can see (i.e., pretty pictures)
(2) Planetesimal belt theory
What we need to know to understand what we see
(3) Planetary perturbations
Some interesting things we can deduce from what we can see

Overview of star and planet formation

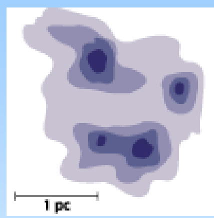

molecular cloud
0Myr

star formation

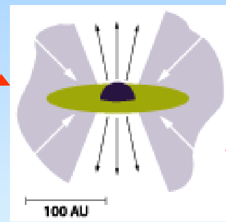

pre-main sequence star
+ protoplanetary disk
1-10Myr

dust
planetesimals
terrestrial planet
gas giant

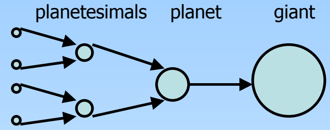

?

planet formation

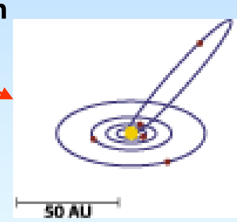

main sequence star
+ planetary system
and/or debris disk
10Myr-10Gyr

Information on planetary systems

(1) Solar system

(2) >180 extrasolar planets

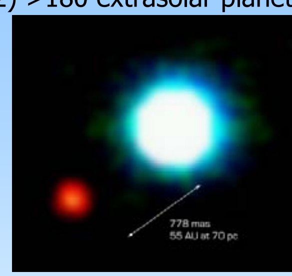

(3) Proto-planetary disk observations

(4) Planet formation models

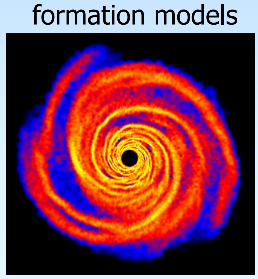

(5) Debris disks

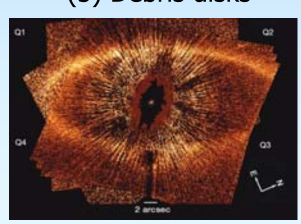

The debris disk of the Solar System

The debris disk of the Solar System is comprised of:

The Kuiper belt

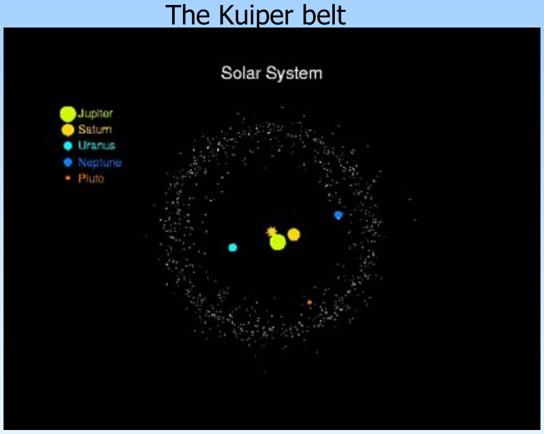

The Asteroid belt

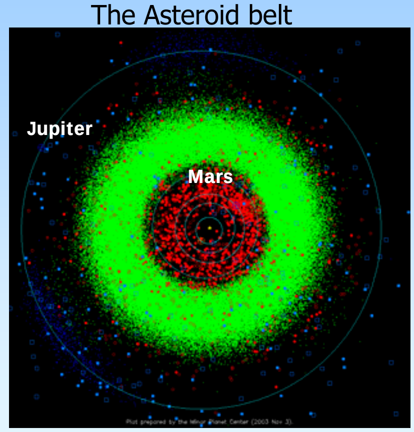

Debris disks are the remnants of the planet formation process, planetesimals which failed to grow into planets.

Discovery of extrasolar debris disks

• IR satellite IRAS detected "**excess**" infrared emission from the nearby 7.8pc main sequence A0V star Vega during routine calibration observations (Aumann et al. 1984)

Excess = more emission than expected from the star alone
SED = Spectral Energy Distribution

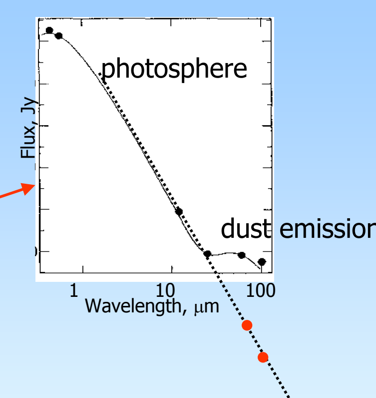

• Excess spectrum fitted by black body at ~85K, interpreted as dust emission in shell with luminosity $f=L_{ir}/L_*=2.5\times10^{-5}$

• Emission marginally resolved at 60μm: FWHM=34" whereas point source would be 25" implying source size of 23" = 180AU at 7.8pc

• This fits with dust heated by star, since $T_{bb} = 278.3\ L_*^{0.25}\ r^{-0.5}$ and so 85K and $L_*=54L_{sun}$ imply radius of ~10″ and source size of 20″

The "big four"

Main sequence stars with excess infrared emission are called "**Vega-like**"

Vega soon joined by 3 more nearby main sequence stars (Gillett 1985):

β Pictoris (A5V at 19.2pc)
Fomalhaut (A3V at 7.8pc)
ε Eridani (K2V at 3.2pc)

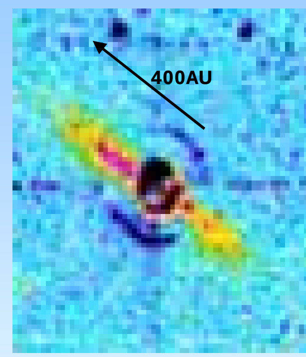

Next big step was when β Pic was imaged using optical coronagraphy showing the dust is in a disk seen edge-on out to 400AU (20") (Smith & Terrile 1984)

Proto-planetary vs debris disks

Proto-planetary disk <10Myr	Debris disk >10Myr
Optically thick	Optically thin

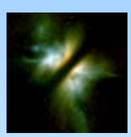

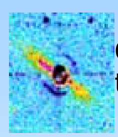

Proto-planetary and debris disks are significantly different

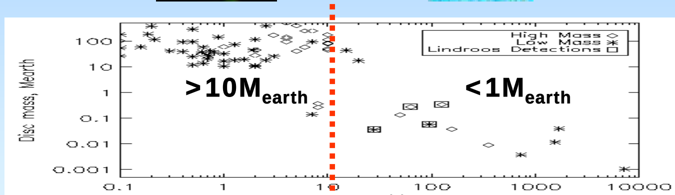

Proto-planetary disk	Debris disk
Dust from 0.1-100AU	Dust at one radius ~30AU
Massive gas disk	No gas
Accretion onto star	No accretion

Debris disk dust not primordial

Debris disks cannot be remnants of the proto-planetary disks of pre-main sequence stars because (Backman & Paresce 1993):

(1) The stars are old, e.g., Vega is **350Myr**

(2) The dust is small (<100μm) (Harper et al. 1984; Parsesce & Burrows 1987; Knacke et al. 1993)

(3) Small grains have short lifetimes due to P-R drag

$t_{pr} = 400\ r^2 / (M_* \beta)$ years,

where $\beta \approx (1100/\rho D)(L_*/M_*)$

e.g., for Vega ($54L_{sun}$, $2.5M_{sun}$, r=90AU, D=100μm, ρ=2700kg/m^3): $\mathbf{t_{pr}=15Myr}$

(4) They also have short lifetimes due to collisions

$t_{coll} = r^{1.5} / 12\ M_{star}^{0.5}\ \tau$ years

e.g., for Vega ($\tau \approx f = 2.5\times10^{-5}$): $\mathbf{t_{coll}=2Myr}$

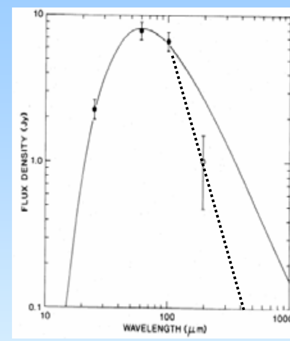

Dust is replenished by the break-up of larger debris with longer P-R drag and collision lifetimes

Discovering debris disks

- Dust is cold, typically 50-120K, meaning it peaks at ~60μm
- Star is hot meaning emission falls off $\propto \lambda^{-2}$
- So most debris disks are discovered in far-IR


Far-IR (space)

- **IRAS (1983)** did all-sky survey at 12,25,60,100μm
- **ISO (1996)** did observations at 25,60,170μm of nearby stars
- **Spitzer (2003-)** currently observing nearby stars at 24,70,160μm
- **Akari (2006-)** currently doing all-sky survey 2-180μm
- **Herschel (2008-)** observations at 60-670μm
- **Spica (2017+)** planned 5-200μm

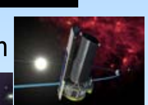

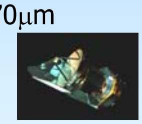

Sub-mm (ground)

- **JCMT, SCUBA2 (2007+)** survey of 500 nearest stars at 850μm
- **ALMA (2008-2012+)** high resolution sub-mm

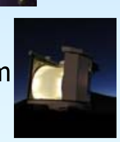


Mid-IR (space)

- **JWST (2013+)**, 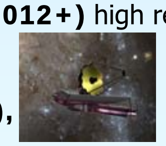 **DARWIN/TPF (2020+)** 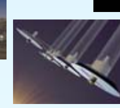

Surveys for debris disks

Survey strategy:

(1) take list of main sequence stars and their positions (e.g., HD catalogue)

(2) look for nearby infrared source (e.g., <60") and get IR flux (e.g., IRAS FSC)

(3) estimate stellar contribution in far-IR (from IRAS F_{12}, or V or B, or 2MASS)

(4) find stars with significant excess

$$\sigma = \frac{[(F_{25}/F_{12})(F_{12*}/F_{25*}) - 1]}{[(\delta F_{12}/F_{12})^2 + (\delta F_{25}/F_{25})^2]^{0.5}} > 3$$

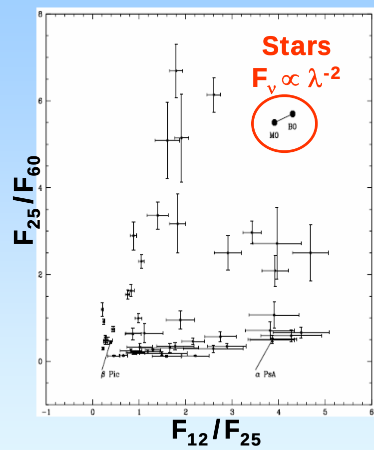

Many papers did this in different ways and there are >901 candidates

What do all these disks tell us?

There are two things observations tell us:

(1) Statistics

How do **debris parameters** correlate with **stellar parameters**?

disk / diskless	spectral type (M_* or L_*),
dust mass (M_{dust})	age (t_*),
or dust luminosity ($f=L_{ir}/L_*$)	metallicity (Z),
dust temperature (T)	presence of planets
or radius (r)	

(2) Detail of individual objects

Images = structure
Spectroscopy = mineralogical features, gas

Dependence on age and spectral type

IRAS:
- 15% of stars have debris (Plets & Vynckier 1999)

ISO:
- Study of 81 main sequence stars within 25pc gave 17% with debris (Habing et al. 2001):
- Dependence on spectral type: A (40%), F (9%), G (19%), K (8%)
- Dependence on age with disk detection rate going up for younger stars, possibly abrupt decline >400Myr (Habing et al. 1999)

Debris disks are more common around early type stars and around young stars

	< 400 Myr		400–1000 Myr		1.0–5.0 Gyr		> 5.00 Gyr	
	tot	disk	tot	disk	tot	disk	tot	disk
A**	10	6	4	0	1	0	0	0
F**	0	0	1	0	17	2	5	0
G**	2	1	0	0	7	0	12	3
K**	3	2	2	0	5	0	12	0
total	15	9	7	0	30	2	29	3

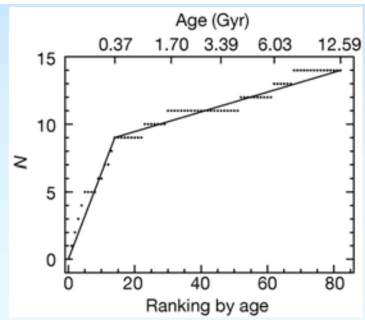

Problem of detection bias

Greaves & Wyatt (2003)

Earlier-type stars have shorter main sequence lives

Disks are found at all ages on the main sequence

No abrupt decline at 400Myr

Solution 1: split samples by spectral type (A stars, FGK stars, M stars)

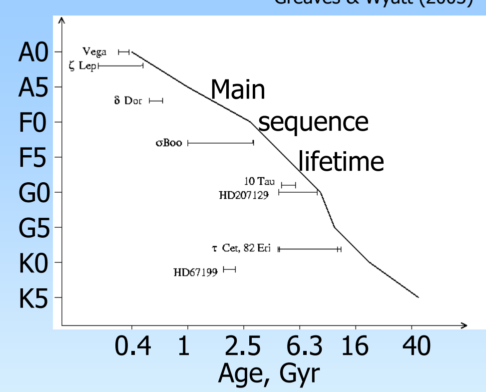

Early-type stars are also more luminous, and it is easier to detect dust around them (remember $T_{bb} = 278.3\, L_*^{0.25}\, r^{-0.5}$); i.e., surveys are sensitive to different disk masses depending on r and L_* as well as λ and threshold sensitivity

Solution 2: survey statistics need well defined thresholds and always need to consider bias

Dust excess evolution

Large Spitzer studies of the 24 and 70μm excesses (F_{tot}/F_*) of A stars found a $\propto t^{-1}$ decline in the upper envelope on timescale of 150Myr at 24μm (Rieke et al. 2005) but longer at 70μm (Su et al. 2006)

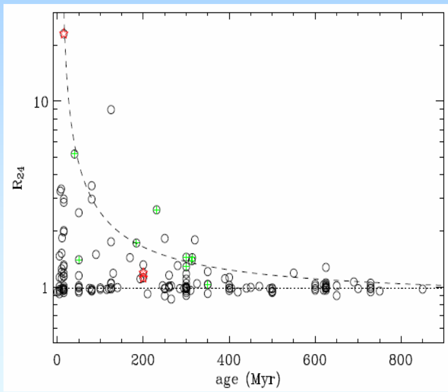

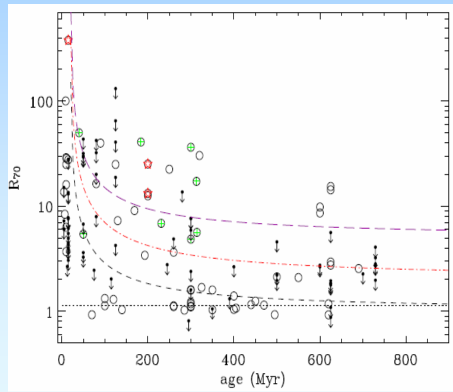

Presence of excess depends on wavelength! Or rather on disk radius

Disk mass and radius evolution

Sub-mm fluxes provide the best measure of disk mass, and show that mass falls off $\propto t^{-1}$ with a large spread of 2 orders of magnitude at any age (Najita & Williams 2005)

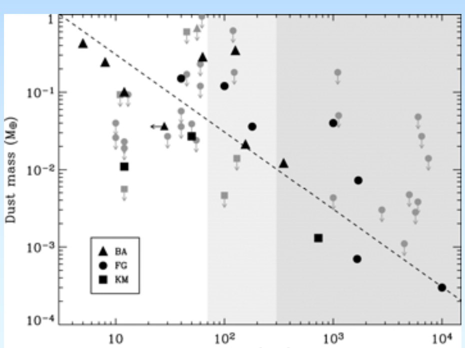

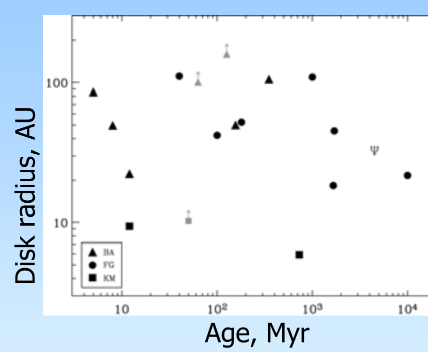

Combined with far-IR fluxes, sub-mm measurements constrain temperature and so radius, showing that there is a large spread in disk radii 5-200 AU at all ages (Najita & Williams 2005)

What is the evolution of individual disks?

We do not know the evolution of individual disks

The bulk observable properties which may evolve with time are: M_{dust} and r
• the population samples suggest that r is constant
• the mass certainly falls, but how?

Models proposed in the literature include:
• steady-state collisional processing,
• stochastic evolution,
• delayed stirring ,
• Late Heavy Bombardment

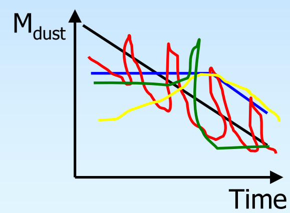

Dependence on metallicity and planets

Of 310 FGK stars <25pc all searched for planets and debris disks (Greaves, Fischer & Wyatt 2006):
• 20 have planets
• 18 have debris detected with IRAS
• 1 has both
• stars with planets are metal-rich (Fischer & Valenti 2005)
• stars with debris disks have same metallicity distribution as all stars

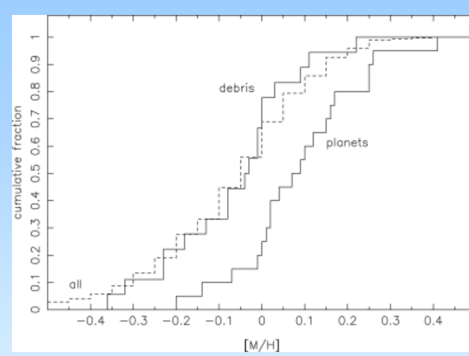

First thought planets and debris could be mutually exclusive (Greaves et al. 2004)

More recent studies with Spitzer show (Beichman et al. 2005):
• 6/26 planet host stars have debris
• Of 84 stars, 4/5 high excess stars have planets
• Planets of debris-planet systems are representative of extrasolar planet sample, though none at <0.25AU

How to Image Debris Disks?

Scattered Light
Optical/Near-IR
Coronagraphy

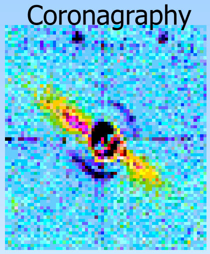

Thermal Emission
Mid-IR

Sub-mm

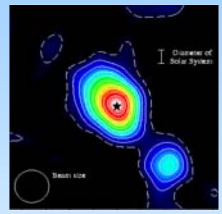

Each technique has its benefits and drawbacks:
e.g., shorter wavelength = higher resolution, but more flux from star

NB in diffraction limit FWHM $\approx \lambda/D$ so that disks of radius r (AU) can be resolved on a telescope D (m) in diameter at wavelength λ (μm) out to
$d_{lim} = 10rD/\lambda$ pc
e.g., 100AU disks can be resolved to 18pc with JCMT
50AU disks to 270pc with Gemini/VLT (more like 100pc with stellar flux)

Debris Disk Image Gallery

Optical/NIR <5μm | Mid-IR 10–25μm | Far-IR 70–200μm | Submillimetre 350μm 450μm 850μm | Millimetre 1.3mm

1984	β Pictoris
1998	HR4796
1998	Fomalhaut
1998	Vega
1998	ε Eridani
2000	HD141569
2004	τ Ceti
2004	HD107146
2005	η Corvi
2005	AU Mic
2005	HD32297
2006	HD53143
2006	HD139664
2006	HD181396
2006+	HD92945

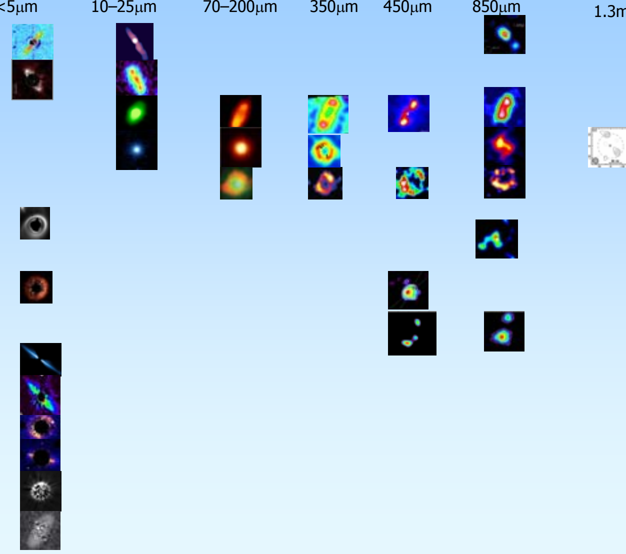

Images of the archetype Vega

Vega is a **350 Myr**-old **A0V** star at **7.8 pc**, and while disk marginally resolved by IRAS, was not until sub-mm images of 1998 that structure seen

850 μm image shows symmetrical **face-on** structure at ~**90 AU** with a mass of **0.01** $\mathbf{M_{earth}}$ (Holland et al. 1998); dust emission dominated by **two clumps** at ~9 arcsec (70 AU)

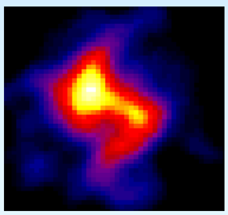

Mm interferometry is sensitive to **small scale** structure, so different resolutions see slightly different structures, but clumps are confirmed

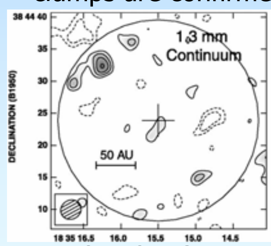

OVRO 1.3 mm
15 nights
(Koerner et al. 2001)

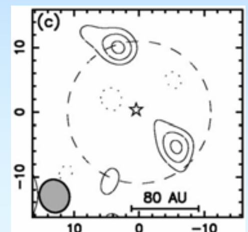

PdB 1.3 mm
23 hours
(Wilner et al. 2001)

Structure is wavelength dependent!

850μm
(Holland et al. 2006)

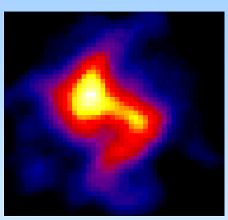

24 and 70μm
(Su et al. 2005)

Surface brightness distribution (Su et al. 2005)

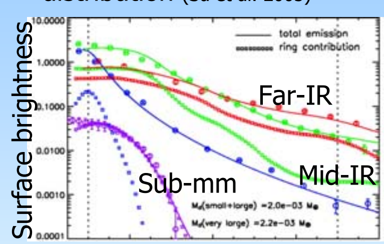

200 400 600 800
Radius, AU

350μm (Marsh et al. 2006)

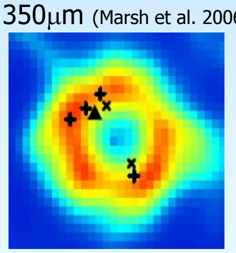

- At 850μm the disk extends to 200AU
- At 24 and 70μm the disk extends to 1000AU
- Dust seen in far-IR implies mass loss of ~2$M_{\oplus}$/Myr and must be transient
- Clumpiness at 350μm is different to 850μm

Fomalhaut's Dust Disk

Because of similar age, spectral type and distance, Vega and Fomalhaut are often compared: Fomalhaut is a **200 Myr**-old **A3V** star at **7.7 pc**

- Sub-mm SCUBA = edge-on **135 AU ring** with mass **0.02 M_{earth}**, clump to SE
- Sub-mm SHARCII = no evidence of clump
- Far-IR = SE ansa brighter
- Mid-IR = some emission from closer to star
- Optical = sharp inner edge, star not at centre of ring

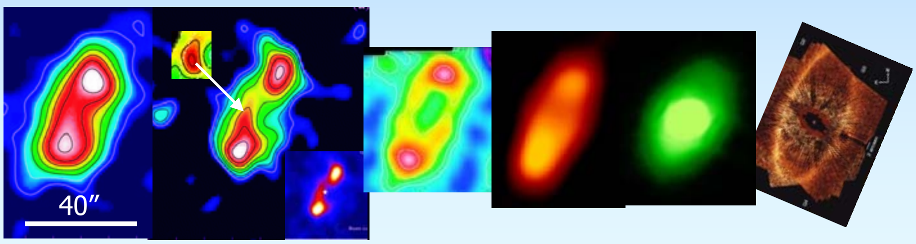

850 µm 450 µm 350µm 70µm 24µm optical

Holland et al. (2003) Marsh et al. (2004) Stapelfeldt et al. (2005) Kalas et al. (2005)

The HR4796 Dust Disk

Debris disks around young stars are brighter and so easier to image
HR4796A (**10 Myr**-old **A0V** star at **67 pc**) is a disk in the TWHydra association

- Mid-IR = edge-on dust ring at **70 AU**, NE brighter than SW
- Near-IR = ring also imaged
- Sub-mm = ring contains **>0.25 M_{earth}** of dust (Greaves et al. 2000)
- Most flux at star is photospheric, but additional dust at 9 AU (Augereau et al. 1999)

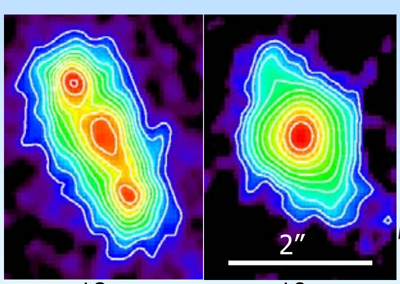

18 µm 10 µm

Telesco et al. (2000)

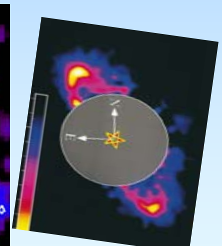

1.1 µm

Schneider et al. (1999)

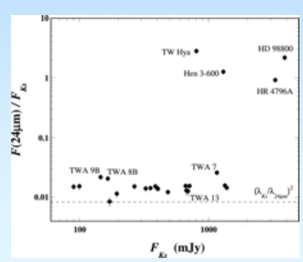

Low et al. (2005)

The inner β Pictoris disk

β Pic is a ~12 Myr A5V star with edge-on disk extending to 1000s of AU and has been imaged in optical to sub-mm

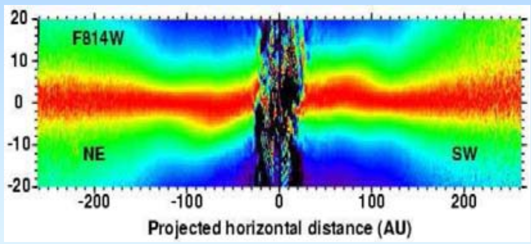

Optical images of inner region show warp at ~100AU (Heap et al. 2000; Krist et al. 2006)

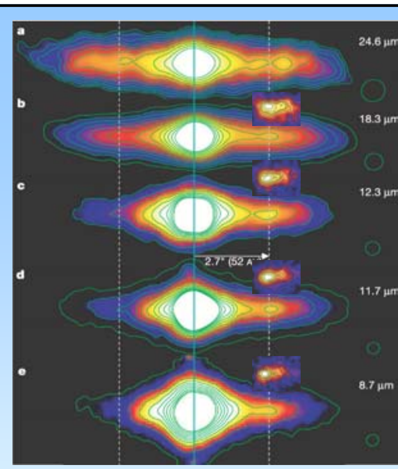

Mid-IR images show a clump of material 52 AU from the star, with temperature indicating grains in the process of radiation pressure blow-out (Telesco et al. 2005)

The outer β Pictoris disk

There is a break in the surface brightness profile at ~7" (130 AU)

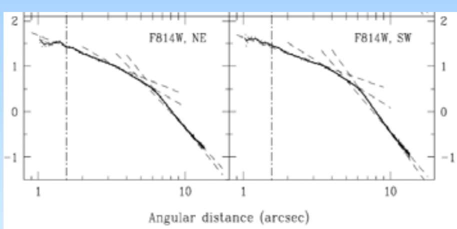

Gas is also detected in β Pic (at low levels, ~gas/dust=0.1) showing keplerian rotation and a similar break in profile indicating this is coincident with the dust (Brandeker et al. 2004)

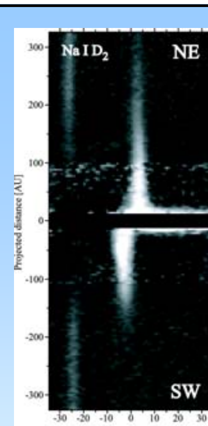

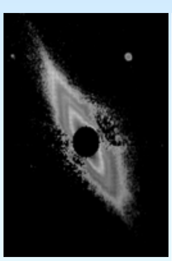

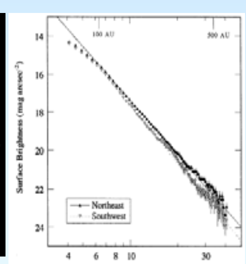

Dust is seen out to 800AU (e.g., Kalas & Jewitt 1995)

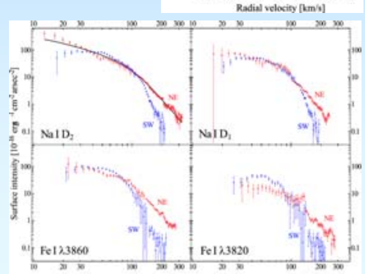

β Pic association (AU Mic)

AU Mic is an M0V star at 10pc in the β Pic association and so is ~12 Myr

It also has an imaged disk which looks remarkably similar to β Pic, since it is:

• edge-on and has a

• turn-over in surface brightness profile

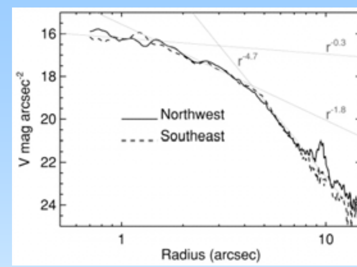

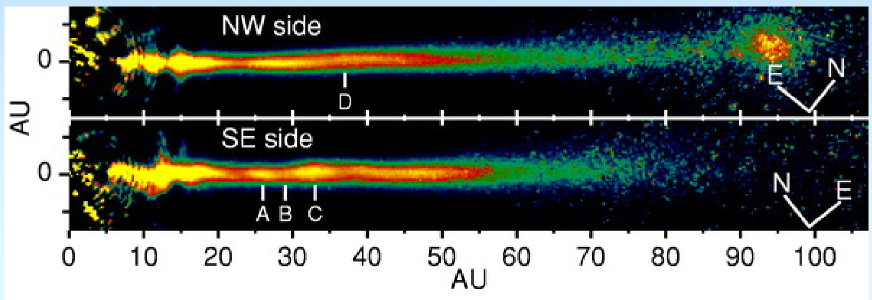

Isolated young stars: HD141569A

• HD141569A is a **5 Myr**-old **B9.5V** star at **99 pc**

• HD141569B and C are M star companions at 1200 AU separation

• Optical coronagraphic imaging from HST shows dust out to 1200 AU, dense rings at 200 and 325 AU with tightly wound spiral structure (Clampin et al. 2003)

• Disk at <200AU marginally resolved mid-IR (Fisher et al. 2000; Marsh et al. 2002)

V band surface brightness

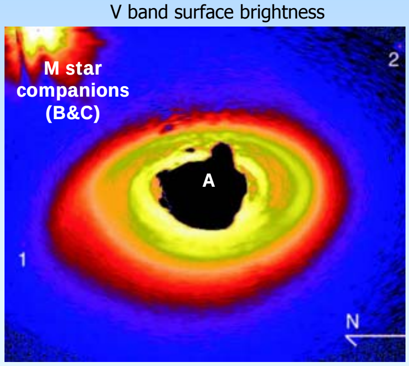

Deprojected surface density

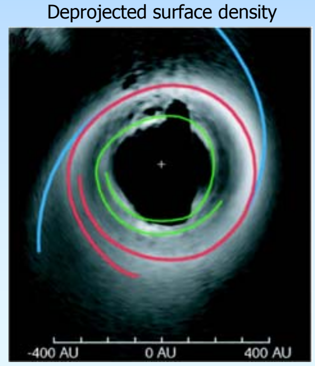

Clampin et al. (2003)

Hot and cold dust around old F star

The 1Gyr old F2V star η Corvi is most notable for its resolved Kuiper Belt, which SCUBA imaging at 450μm shows is near edge-on with a radius of ~100AU and central cavity (Wyatt et al. 2005)

The SED shows presence of hot dust, which mid-IR imaging confirms placing location at <10AU

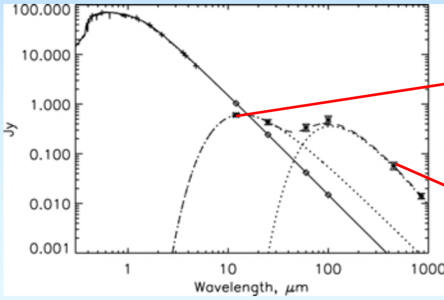

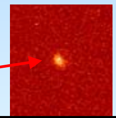

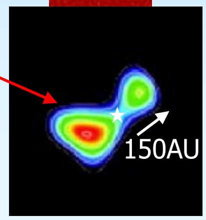

The "Hale-Bopp" star HD69830

Only 2% of stars have hot dust <10AU (Bryden et al. 2006), one of which is 2Gyr old K0V star HD69830

A mid-IR spectrum similar to that of Hale-Bopp with a temperature of ~400K, shows dust is concentrated at 1AU (Beichman et al. 2005)

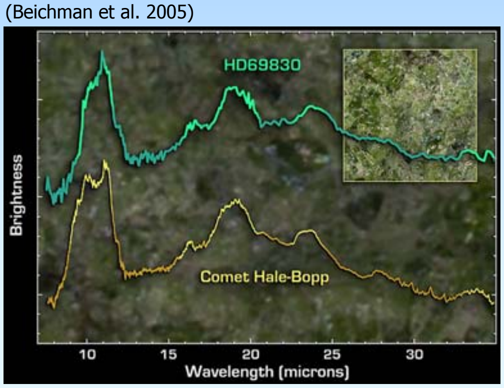

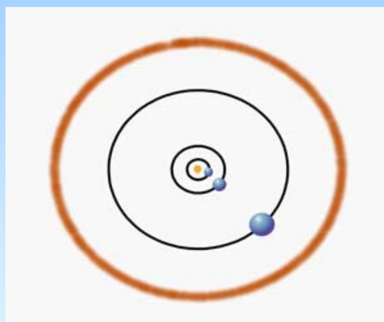

It was also recently found to have 3 Neptune mass planets orbiting at 0.08, 0.16 and 0.63 AU on nearly circular orbits (Lovis et al. 2006)

Very unusual to have dust at 1AU at 2Gyr implying it is transient (Wyatt et al. 2007)

Old debris disks: ε Eridani

- ε Eridani is an **800 Myr**-old **K2V** star at **3.2 pc**
- 850 μm image (**30hr**) shows 25º from face-on, slightly offset, dust ring at **60 AU** with a mass of **0.01 M_{earth}** (Greaves et al. 1998; 2005)
- Emission dominated by **3 clumps** of asymmetric brightness
- 1″/yr proper motion detected, possible rotation of structure (Poulton et al. 2006)
- planet at 3.4 AU with e=0.6 (Hatzes et al. 2000)

1997

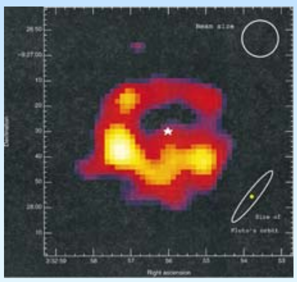

Greaves et al. (1998)

1997-2003 | 1997 (col), 2003 (cont)

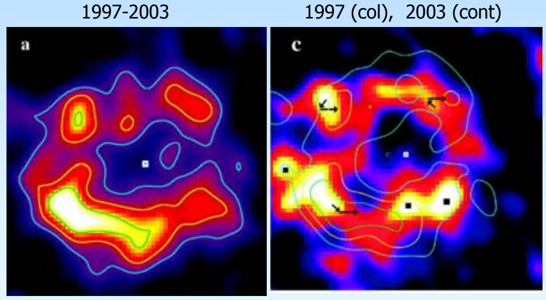

Greaves et al. (2005)

Old Debris Disks: τ Ceti

- τ Ceti is a 7.2 Gyr G8V star at 3.6 pc
- Imaging at 850 μm has confirmed the presence of an inclined debris disk with a radius ~55 AU, and a dust mass 5 x 10^{-4} M_{earth}
- Thus it has at least ten times more mass than the Kuiper Belt ~10^{-5} M_{earth}
- The only solar-type (age and spectral type) star with confirmed debris disk

850 μm (Greaves et al. 2004)

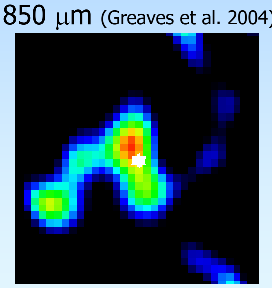

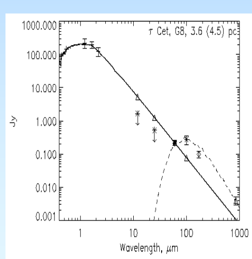

K5-G9 Stars within 4 pc

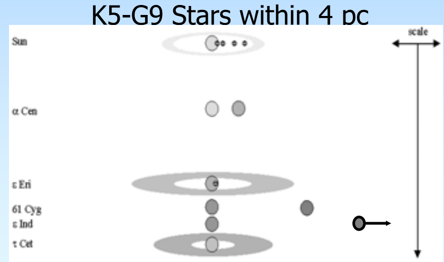

Of the six nearest K5-G9 stars, three are binary systems, two have massive debris disks, and one, the Sun, has a tenuous debris disk

Background galaxies in sub-mm

Clumps in sub-mm images are ubiquitous, and are usually assumed to be background galaxies (aka SCUBA galaxies), which have number counts from blank field surveys:

620 $F_{850\mu m}$>5mJy sources per square degree (Scott et al. 2002)
2000 $F_{450\mu m}$>10mJy sources per square degree (Smail et al. 2002)

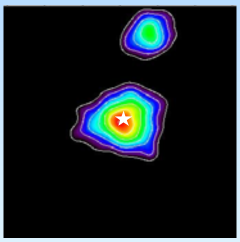

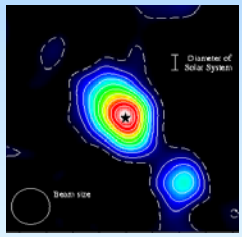

However they appear so often near debris disks (especially 19mJy source near β Pic) that perhaps some are related objects

Debris disk studies provide deep surveys for background galaxies in relatively unbiased way (all sky), and candidates can be easily followed up with AO imaging because of proximity to guide/reference star

Bogus debris disks

Imaging weeded out bogus debris disks, stars with IRAS excesses that come from background objects:

- 55 Cancri - bounded by three galaxies (Jayawardhana et al. 2002)
- HD123160 - giant star with nearby galaxy (Kalas et al. 2002; Sheret, Dent & Wyatt 2003)
- HD155826 - background carbon star (Lisse et al. 2002)

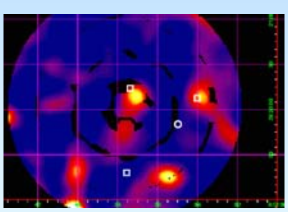

55 Cancri at 850 μm (and R)
(Jayawardhana et al. 2002)

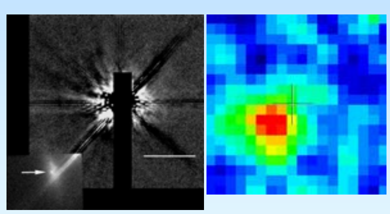

HD123160 at K and 850 μm
(Kalas et al. 2002) (Sheret, Dent & Wyatt 2003)

HD155826
at 11.7 μm
(Lisse et al. 2002)

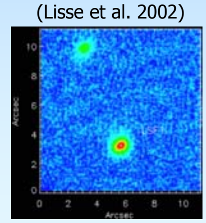

Nearby cirrus

Kalas et al. (2002)

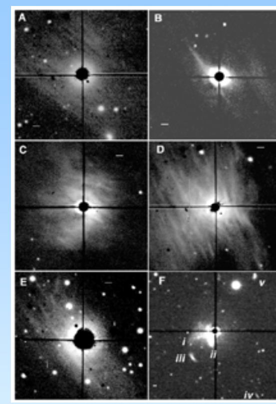

Some stars are interacting with nearby cirrus

Optical images show diffuse nebulosity around the stars with a stripy pattern reminiscent of structure in cirrus seen in the Pleiades

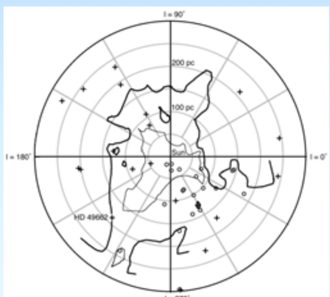

The Sun is situated in the local bubble (<100pc, see NaD absorption contours) meaning the local ISM is too diffuse for this kind of interaction, but more distant debris disk candidates may be bogus

HD32297

One of the imaged debris disks is associated with a wall of interstellar gas

This is an 8Myr A0V star at 113pc with a $L_{ir}/L_{*}=2.7\times10^{-3}$ disk to 400AU imaged in near-IR, with distinct asymmetry in nebulosity to 1680 AU at slightly different position angle (15^{o}) in optical

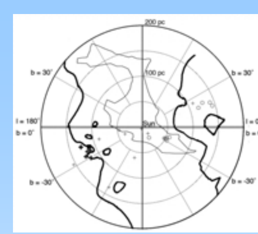

Optical R band image (Kalas et al. 2005)

NICMOS near-IR image (Schneider et al. 2005)

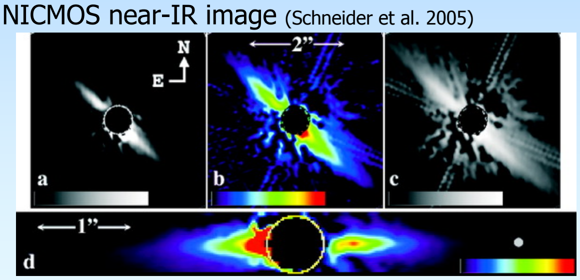

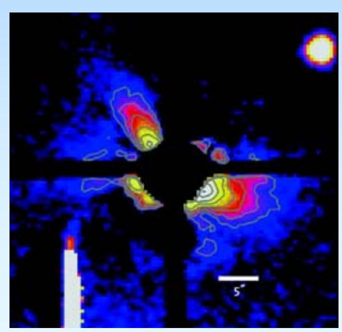

The interaction of ISM on the disk (eg., sandblasting) is still unknown

Models have to explain...

(1) Radial structure (2) Asymmetric structure (3) Evolution

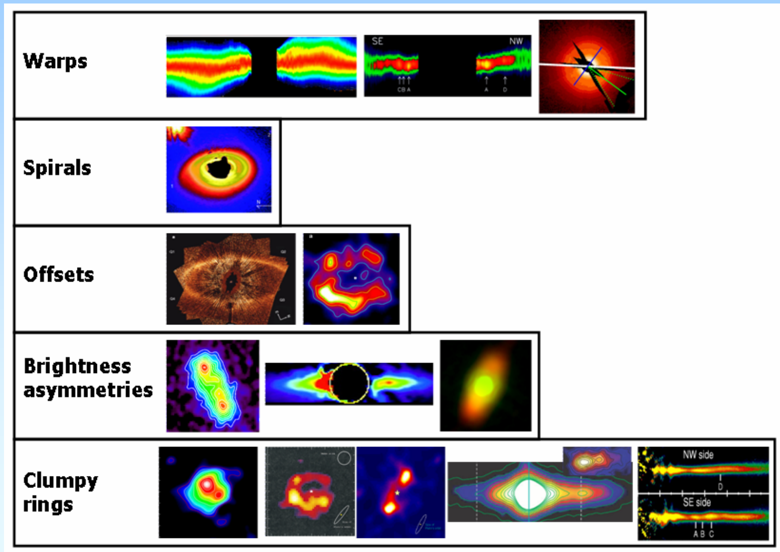

Planetesimal belt theory

In order to interpret the observations we need a model of the underlying physics of a debris disk, and of the physics which affects their observational properties

Here I will build up a simple analytical model for the physics of planetesimal belts, based on the models developed in

Wyatt et al. 1999, ApJ, 529, 618
Wyatt 1999, Ph.D. Thesis, Univ. Florida
Wyatt & Dent 2002, MNRAS, 348, 348
Wyatt 2005, A&A, 452, 452
Wyatt et al. 2007, ApJ, 567, in press

copies of which you can find on my website

http://www.ast.cam.ac.uk/~wyatt

The planetesimal belt

Consider planetesimals orbiting the star at a distance r in a belt of width dr

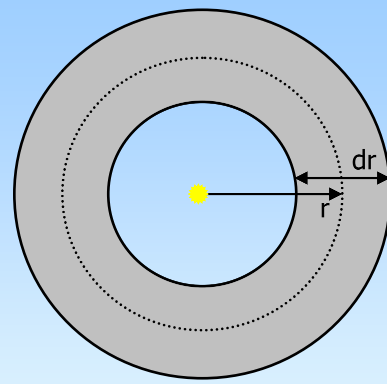

Face-on area of belt is:
2π r dr

Volume of belt is:
$4\pi r^2 I$ dr

Cross-sectional area of material in belt:
σ_{tot} in AU^2

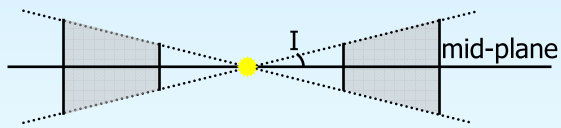

Surface density of the belt:
$\tau_{eff} = \sigma_{tot} / (2\pi r\, dr)$, AU^2/AU^2

Gravity

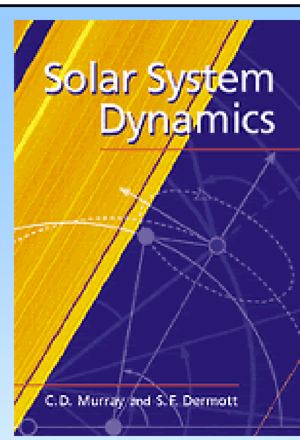

- The dominant force on all planetesimals is gravitational attraction of star

- The force between two massive bodies, M_1 and M_2 is given by
  $F = GM_1M_2/r^2$,
  where $G=6.672\times10^{-11}$ Nm^2kg^{-2}

- Expressing in terms of vector offset of M_2 from M_1, **r** gives the equation of motion as
  $d^2\mathbf{r}/dt + \mu\mathbf{r}/r^3 = 0$,
  where $\mu=G(M_1+M_2)$

- Which can be solved to show that the orbit of M_2 about M_1 is given by an ellipse with M_1 at the focus (or, e.g., a parabola)

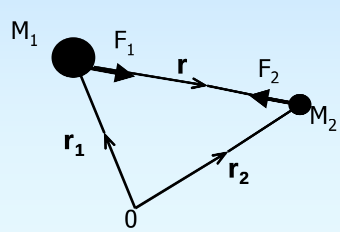

Orbits in 2D

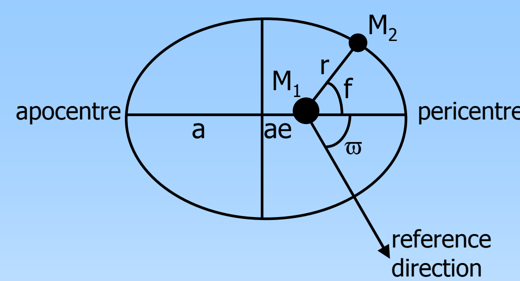

- The orbit is given by:
  $r = a(1-e^2)/[1 + e \cos(f)]$,
  a=semimajor axis,
  e=eccentricity,
  f=true anomaly

- Angular momentum integral:
  $h = r^2 df/dt = [\mu a(1-e^2)]^{0.5} = \text{const}$
  Orbital period $t_{per} = 2\pi(a^3/\mu)^{0.5}$

- Energy integral:
  $0.5v^2 - \mu/r = \text{const} = C = -0.5\mu/a$
  $V_p = [(\mu/a)(1+e)/(1-e)]^{0.5}$
  $V_a = [(\mu/a)(1-e)/(1+e)]^{0.5}$

- Mean angles:
  Mean motion: $n = 2\pi/t_{per}$
  Mean anomaly: $M = n(t-\tau)$
  Mean longitude: $\lambda = M + \varpi$

- Eccentric anomaly, E
  $\tan(E/2) = [(1-e)/(1+e)]^{0.5}\tan(f/2)$
  $M = E - e\sin(E)$

$t_{per} = (a^3/M_*)^{0.5}$ yrs and $v_k = 30(M_*/a)^{0.5}$ km/s, where M_* is in M_{sun} and a in AU

Orbits in 3D

- In 3D just need to define the **orbital plane**, which is done with:
  I = inclination
  Ω = longitude of ascending node

- Also need to define the direction to pericentre:
  ω = argument of pericentre
  ϖ = longitude of pericentre = Ω+ω

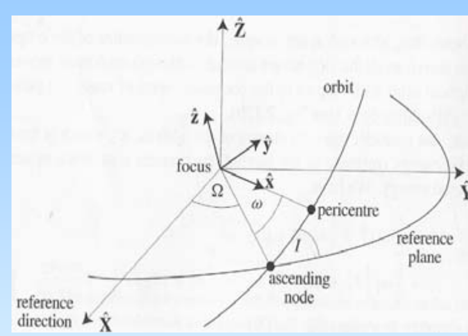

- So, the orbit is defined by five variables: **a, e, I,** Ω and ϖ (or ω)

- One time dependent variable describes location in orbit: λ (or f, M or E)

- Method for converting between [**X,Y,Z,V_x,V_y,V_z**] and [**a,e,I,Ω,ϖ,λ**] is given in Murray & Dermott (1999)

Size distributions

Planetesimals have a range of sizes

Define a size distribution such that n(D) dD is the number of planetesimals in size range D to D+dD

$n(D) = K D^{2-3q}$ between D_{min} and D_{max}

Assuming spherical particles so that $\sigma=\pi D^2/4$ gives

$\sigma_{tot} = [0.25K\pi/(5-3q)][D_{max}^{5-3q} - D_{min}^{5-3q}]$

$\sigma(D_1,D_2) = \sigma_{tot} [(D_1/D_{min})^{5-3q} - (D_2/D_{min})^{5-3q}]$

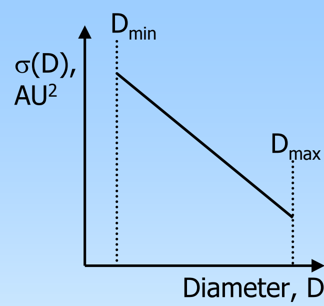

Similar relations for $m(D_1,D_2)$ (assuming $m=\pi D^3\rho/6$) and $n(D_1,D_2)$ meaning that number mass and area in the distribution is dominated by large or small particles depending on q

q	$n(D_1,D_2)$	$\sigma(D_1,D_2)$	$m(D_1,D_2)$
<1	large	large	large
1 to 5/3	small	large	large
5/3 to 2	small	small	large
>2	small	small	small

Collisional cascade

When two planetesimals collide (an **impactor** D_{im} and **target** D) the result is that the target is broken up into fragments with a range of sizes

If the outcome of collisions is self-similar (i.e., the size distribution of fragments is the same for the the same D_{im}/D regardless of whether D=1000km or 1μm), and the range of sizes infinite, then the resulting size distribution has an exponent (Dohnanyi et al. 1969; Tanaka et al. 1996)

q = 11/6

This is known as a **collisional cascade** because mass is flowing from large to small grains

Shattering and dispersal thresholds

The outcome of a collision depends on the **specific incident kinetic energy**
$Q = 0.5\,(D_{im}/D)^3\,v_{col}^2$

Shattering threshold, Q_S^*: energy for largest fragment after collision to have $(0.5)^{1/3}D$
- Impacts with $Q<Q_S^*$ result in cratering (ejection of material but planetesimal remains intact)
- Impacts with $Q>Q_S^*$ result in catastrophic destruction

Dispersal threshold, Q_D^*: energy for largest fragment after reaccumulation to have $(0.5)^{1/3}D$

Strength regime: $Q_D^* \approx Q_S^*$ for D<150m
Gravity regime: $Q_D^* > Q_S^*$ for D>150m

Catastrophic collisions

The only study which generalises the outcome of collisions for a range of energies of interest in debris disks is the SPH simulations of Benz & Asphaug (1999)

They parametrised Q_D^* as a function of composition (basalt/ice) and for a range of v_{col} (two which can be interpolated between, or extrapolated)

For catastrophic collisions: $Q>Q_D^*$ so
$D_{im}/D > X_{tc} = (2Q_D^*/v_{col}^2)^{1/3}$

For collisions at v_{col}=1 km/s this means
X_{tc}=0.01 to 1

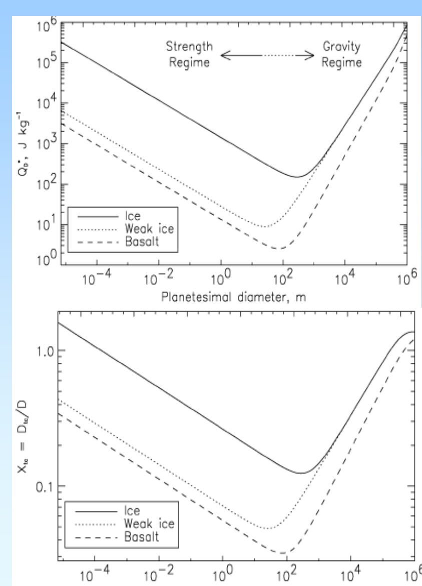

Catastrophic collision rate

The rate of impacts onto a planetesimal of size D from those in the size range D_{im} to $D_{im} + dD_{im}$ is $R_{col}(D,D_{im})dD_{im}$ (Opik 1950) where

$R_{col}(D,D_{im}) = f(D,D_{im})\, \sigma(r,\theta,\phi)\, v_{rel}$

where

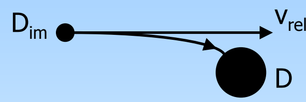

$v_{rel} = f(e,I)v_k$ [NB $f(e,I) = (1.25e^2 + I^2)^{0.5}$]

$\sigma(r,\theta,\phi) = \sigma_{tot}/(4\pi r^2 dr I)$

$f(D,D_{im})dD_{im} = [\sigma(D_{im})/\sigma_{tot}][1+(D/D_{im})]^2[1+(v_{esc}(D,D_{im})/v_{rel})^2]$

is the fraction of σ_{tot} that the planetesimal sees

$v_{esc}^2(D,D_{im}) = (2/3)\pi G\rho[D^3+D_{im}^3]/(D_{im}+D)$

is escape velocity

Mean time between catastrophic collisions

$t_{cc}(D) = t_{per}(r\, dr/\sigma_{tot})[2I/f(e,I)]/f_{cc}(D)$

where

$f_{cc}(D) = \int_{D_{tc}(D)}^{D_{max}} f(D,D_{im})\, dD_{im}$

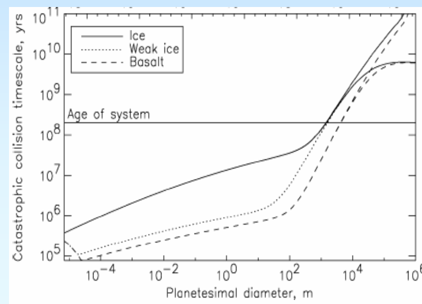

Simplified collision times

For a disk of same sized particles, $f_{cc}(D) = 4$:

$t_{cc} = t_{per} / [4\pi\tau_{eff}[1+1.25(e/I)^2]^{0.5}] \approx t_{per} / 4\pi\, \tau_{eff}$

If gravitational focussing can be ignored, then $f_{cc}(D)$ can be solved:

$f_{cc}(D) = (D_{min}/D)^{3q-5}\, G(q,X_c)$

$G(q,X_c) = [(X_c^{5-3q}-1)+(6q-10)(3q-4)^{-1}(X_c^{4-3q}-1)+(3q-5)(3q-3)^{-1}(X_c^{3-3q}-1)]$

$t_{cc}(D) = (D/D_{min})^{3q-5}\, t_{per} / [G(q,X_c)\pi\tau_{eff}[1+1.25(e/I)^2]^{0.5}]$

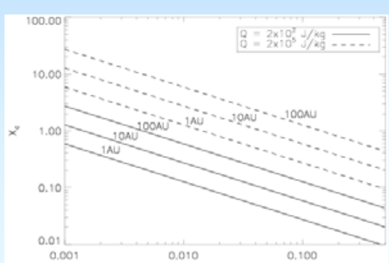

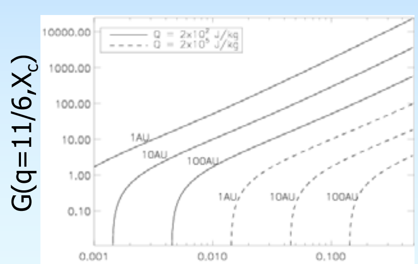

Actual outcome

Collisions do not either destroy a planetesimal or not

The largest fragment in a collision, $f_{lr} = M_{lr}/M$ is given by

$Q < Q_D^*$ $\quad f_{lr} = 1 - 0.5\,(Q/Q_D^*)$

$Q > Q_D^*$ $\quad f_{lr} = 0.5(Q_D^*/Q)^{1.24}$

The size distribution of the fragments can then be constrained by considering that the total mass of remaining fragments = $M\text{-}M_{lr}$

For example, experiments show the fragments to have a size distribution with an exponent

$q_c \approx 1.93$

(although results get 1.83-2.17, and there may be a knee in the size distribution at 1mm)

This means that the second largest fragment must have size:

$D_2/D = [(1\text{-}f_{lr})(2/q_c\text{-}1)]^{1/3}$

We now know the outcome and frequency of all collisions in a planetesimal disk

Real cascade size distribution

The size distribution is not that of an infinite collisional cascade:

- The largest planetesimals are only so big, D_{max}, so mass is lost from the cascade
- The cascade is not self-similar, since X_{tc} is a function of D
- The smallest dust is removed faster than it is produced in collisions and so its number falls below the q=11/6 value

Radiation forces

• Small grains are affected by their interaction with stellar radiation field (Burns et al. 1979)

• This is caused by the fact that grains remove energy from the radiation field by absorption and scattering, and then re-radiate that energy in the frame moving with the particle's velocity:

$F_{rad}=(SA/c)\,Q_{pr}\,[\,[1-2(dr/dt)/c]\mathbf{r} - r(d\theta/dt)\boldsymbol{\theta}\,]$
= radiation pressure ($\mathbf{r}$) +
Poynting-Robertson drag (θ)

• The drag forces are defined by the parameter β which is a function of particle size (D):
$\beta=F_{rad}/F_{grav}=C_r(\sigma/m)\langle Q_{pr}\rangle_{T*}(L_*/L_{sun})(M_{sun}/M_*)$,
where C_r = 7.65x10^{-4} kg/m^2

• For large spherical particles:
$\beta = (1150/\rho D)(L_*/L_{sun})(M_{sun}/M_*)$

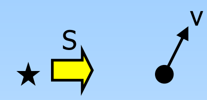

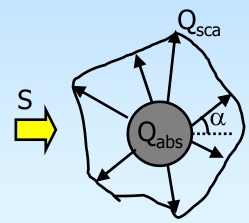

$Q_{pr}=Q_{abs}+Q_{sca}[1-\langle\cos(\alpha)\rangle]$

Radiation pressure

• The radial component is called radiation pressure, and essentially causes a particle to "see" a smaller mass star by a factor (1-β), so that particles with β>1 are not bound and leave the system on hyperbolic trajectories

• This means that a small particle orbiting at "a" has a different orbital period to that of larger objects: $t_{per} = [a^3/M_*(1-\beta)]^{0.5}$ which also moves the locations of resonances etc

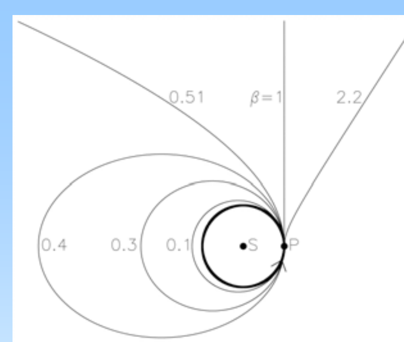

Most important consequence is the change in orbital elements for particles released from a large object (can be derived from the 2D orbits from position and velocity at P the same):

$a_{new}=a(1-\beta)[1-2\beta[1+e\cos(f)][1-e^2]^{-1}\,]^{-1}$
$e_{new}=[e^2+2\beta e\cos(f)+\beta^2]^{0.5}/(1-\beta)$
$\varpi_{new}-\varpi\ =f-f_{new}=\arctan[\beta\sin(f)[\beta\cos(f)+e]^{-1}]$

which means particles are unbound if β>0.5

Poynting-Robertson drag

• Poynting-Robertson drag causes dust grains to spiral into the star while at the same time circularising their orbits ($dI_{pr}/dt=d\Omega_{pr}/dt=0$):

$da_{pr}/dt = -(\alpha/a)(2+3e^2)(1-e^2)^{-1.5} \approx -2\alpha/a$

$de_{pr}/dt = -2.5(\alpha/a^2)e(1-e^2)^{-0.5} \approx -2.5e\alpha/a^2$

where $\alpha = 6.24\times10^{-4}(M_*/M_{sun})\beta$ AU^2/yr

• So time for a particle to migrate in from a_1 to a_2 is

$t_{pr} = 400(M_{sun}/M_*)[a_1^2 - a_2^2]/\beta$ years

• On their way in particles can become trapped in resonance with interior planets, or be scattered, or accreted, or pass through secular resonances…

• Large particles move slower, and so suffer no migration before being destroyed in a collision with another large particle ($t_{pr}\propto D$ whereas $t_{cc}\propto D^{0.5}$), with the transition for which P-R drag is important

$\beta_{pr} = 5000\tau_{eff}(r/M_*)^{0.5}$

Collisions vs P-R drag

Consider a belt of planetesimals at r_0 which is producing dust of just one size

That dust population then evolves due to collisions: $t_{col} = t_{per}/4\pi\tau_{eff}$

P-R drag: $dr_{pr}/dt = -2\alpha/r$

The continuity equation is:

$d[n(r)dr_{pr}/dt]/dr = -n(r)/t_{col}$

which can be expanded to:

$dn/dr - n/r = Kn^2r^{-1.5}$

and solved using Bernoulli's equation:

$\tau_{eff}(r) = \tau_{eff}(r_0)[1+4\eta_0(1-(r/r_0)^{0.5})]^{-1}$

where $\eta_0 = 5000\tau_{eff}(r_0)[r_0/M_*]^{0.5}/\beta = t_{pr}/t_{col}$

Note that the same equation implies that particles evolving due to P-R drag have a size distribution $n(D) \propto n_s(D)D$

If $\eta_0 >> 1$ then dust remains confined to the planetesimal belt

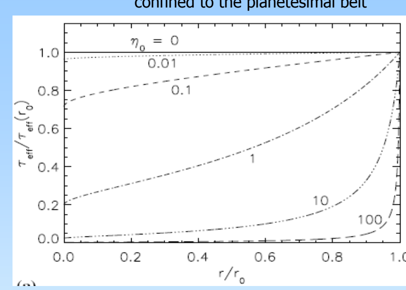

Regardless of $\tau_{eff}(r_0)$, the maximum optical depth at r=0 is $5\times10^{-5}\beta[M_*/r_0]^{0.5}$

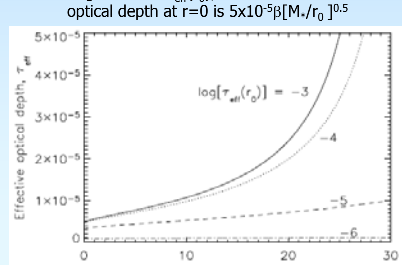

Disk particle categories

This motivates a division of disk into particle categories depending on size:

- $\beta << \beta_{pr}$ **(large):** planetesimals confined to belt
- $\beta \approx \beta_{pr}$ **(P-R drag affected):** depleted by collisions before reaching star
- $\beta_{pr} < \beta < 0.5$ **(P-R drag affected):** largely unaffected by collisions (evaporate at star)
- $0.1<\beta<0.5$ (β **critical**): bound orbits, but extending to larger distances than planetesimals
- $\beta>0.5$ (β **meteoroid**): blown out on hyperbolic orbits as soon as created

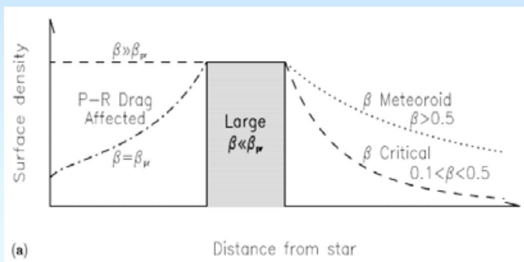

Which categories exist in a disk depends on the disk density

P-R drag dominated disks

A significant P-R drag affected grain population is only expected in tenuous disks for which
$\tau_{eff} < \tau_{effPR} = 10^{-4} [M_*/r]^{0.5}$
since then $\beta_{pr}<0.5$

Such disks have a size distribution with area dominated by grains $\sim\beta_{pr}$ in size

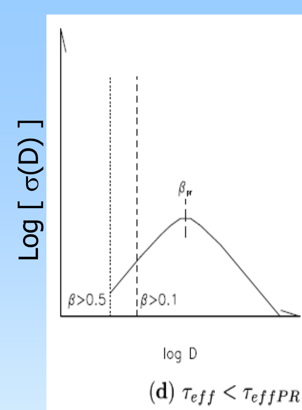

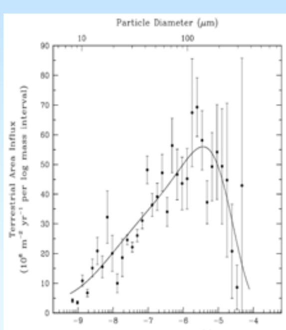

The asteroid belt and zodiacal cloud are examples of this regime, since $\tau_{eff} \approx 10^{-7}$ meaning the material in the asteroid belt should be concentrated in particles $D_{pr}\sim500\mu m$ with smaller particles dominating closer to the Sun (100-200μm dominate accretion by Earth, (Love & Brownlee 1993)

Collision dominated disks

The majority of debris disks have

$\tau_{effPR} < \tau_{eff} < 0.1$

meaning that P-R drag is insignificant, but that grains getting blown out by radiation pressure are not created quickly enough for them to contribute much to σ_{tot}

Such disks have a size distribution with area dominated by grains β~0.1-0.5 in size and so may have a large β critical component

Since grains with β>0.5 are removed on orbital timescales (e.g., consider that when β=1 velocity is constant so one orbital time moves grains from r to 6.4r), they become important when $t_{col} < t_{per}$ and so $\tau_{eff} > 0.1$ (note that such disks are becoming optically thick)

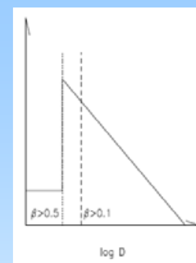

(c) $\tau_{effPR} < \tau_{eff} < 0.1$

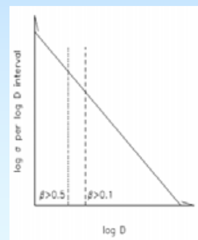

(b) $\tau_{eff} > 0.1$

Wavy size distribution: bottom end

We expect the size distribution to differ from q=11/6 for small sizes because of their removal by radiation forces

• a sharp cut-off causes a wave, since β critical grains should be destroyed by β>0.5 grains (Thebault, Augereau & Beust 2003) [the period of the wave is indicative of X_{tc}]

• if a large number of blow-out grains do exist, however, their large velocities can significantly erode the β critical population (Krivov, Mann & Krivova 2000)

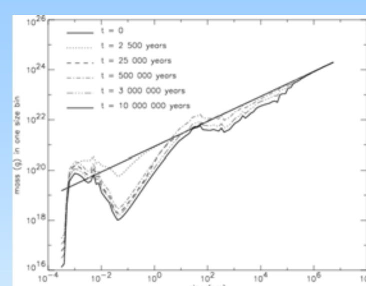

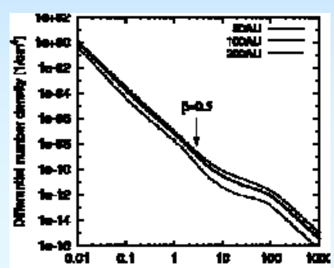

Wavy size distributions: middle / top

The transition from strength to gravity scaling also causes a wave in the size distribution

• If $Q_D^* \propto D^s$ then equilibrium size distribution has (O'Brien & Richardson 2003):

- $q>11/6$ if $s<0$ (strength regime)
- $q<11/6$ if $s>0$ (gravity regime)

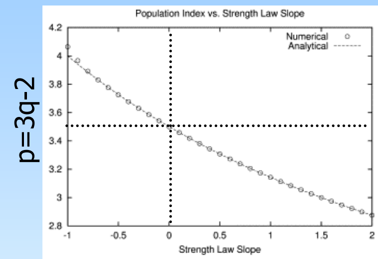

• The transition between the two size distributions causes a wave in the distribution (Durda et al. 1998), and asteroid belt size distribution well fitted thus constraining Q_D^* vs D and concluding that D>120km are primordial (Bottke et al. 2005)

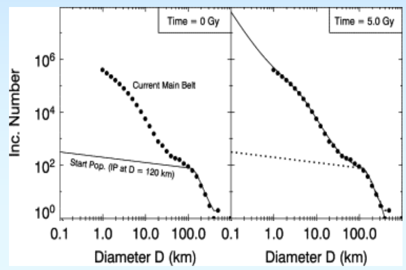

Simple evolution model

The cut-off in the size distribution at D_{max} means no mass input at the top end of the cascade resulting in a net decrease of mass with time:

$$dM_{tot}/dt = - M_{tot}/t_{col}$$

where M_{tot} is dominated by grains of size D_{max} which, assuming a size distribution described by q, have a lifetime of

$$t_{col} = r^{1.5} M_*^{-0.5} (\rho r dr D_{max}/M_{tot})\ (12q-20)(18-9q)^{-1}[1+1.25(e/I)^2]^{-0.5}/G(q,X_c)$$

This can be solved to give:

$$M_{tot}(t) = M_{tot}(0)\ [\ 1 + t/t_{col}(0)\ ]^{-1}$$

In other words, mass is constant until a significant fraction of the planetesimals of size D_{max} have been catastrophically destroyed at which point it falls of $\propto 1/t$

Dust evolution: collision dominated

Forgetting waviness, the size distribution of dust in a collisionally dominated disk is proportional to the number of large planetesimals and so is the area of the dust (which is what is seen):

$$\sigma_{tot} = M_{tot}\,(18\text{-}9q)(6q\text{-}10)^{-1}\rho^{-1}(D_{min}/D_{max})^{3q-6}D_{min}^{-1}$$

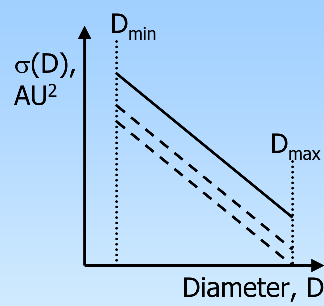

A common way of expressing this observationally is the fractional luminosity of the dust, which if you assume the black body grains:

$$f = L_{ir}/L_* = \sigma_{tot} / 4\pi r^2$$

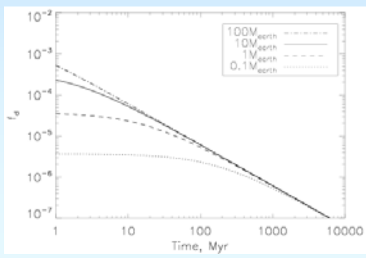

The mass (or f) of a disk at late times is independent of the initial disk mass; i.e., there is a maximum possible disk luminosity at a given age:

$$f_{max} = r^{1.5}M_*^{-0.5}(dr/4\pi r t_{age})(D_{min}/D_{max})^{5-3q} * 2[1+1.25(e/I)^2]^{-0.5}/G(q,X_c)$$

Evolution of size distribution

The evolution of the size distribution can be followed using schemes where, in each timestep, mass is lost from each size bin due to destructive collisions with other planetesimals, and mass is gained due to the fragmentation of larger particles

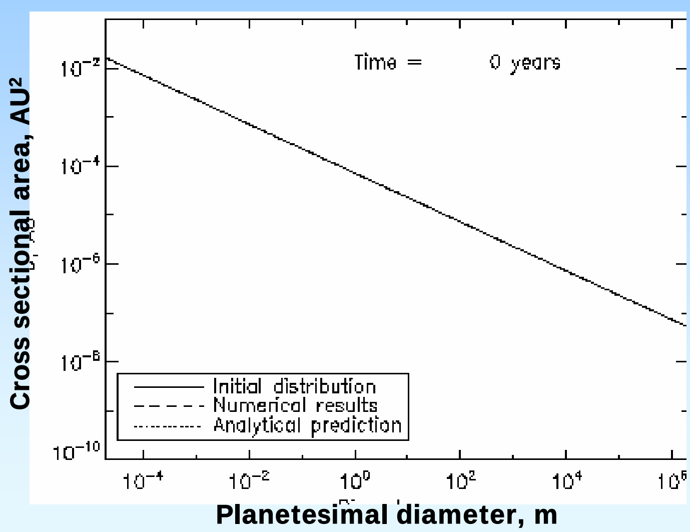

Dust evolution: blow-out grains

The exact number of grains below the radiation pressure blow-out limit depends on how many are created in different collisions:
- planetesimals with dusty regoliths may release large quantities in collisions
- tiny grains may condense after massive collision
- small grains have higher velocities and so preferentially escape in gravity regime

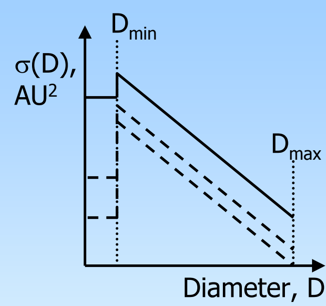

Regardless, since their production rate is $\propto M_{tot}^2$ and their loss rate is constant, their number will fall $\propto M_{tot}^{-2}$ and so $\propto t^{-2}$

Massive collisions

The collision rate, R_{col}, gives a mean time between collisions, t_{col}, which the steady state model can be used to work out the number of collisions that occur between objects of size D to D+dD and D_{im} and $D_{im}+dD_{im}$

However, the actual number of collisions in the timestep is a random number and should be chosen by Poisson statistics (Durda et al. 1997)

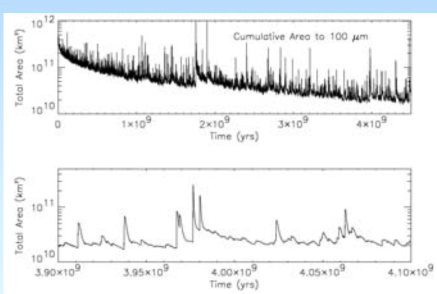

Important for collisions between largest objects which happen infrequently, but have large impact on disk

Models show asteroid belt evolution is punctuated by increases in dust when large asteroids are destroyed

This is not usually the case for debris disks for which single asteroid collisions do not produce a detectable signature

Steady state vs stochastic evolution

That is the steady state model for planetesimal belt evolution, and explains the observed $\propto t^{-1}$ evolution

Several mechanisms have been proposed to cause non-equilibrium evolution, including:

- close passage of nearby star (Kenyon & Bromley 2002)
- formation of Pluto-sized object in the disk (Kenyon & Bromley 2004)
- passge through dense patch of ISM (Arytmowicz & Lubow 1997)
- dynamical instability in the disk (e.g., LHB type event; Gomes et al. 2005)
- sublimation of supercomet (Beichman et al. 2005)
- massive collision between two asteroids (Wyatt & Dent 2002)

All of these models can be interpreted in terms of the steady state model: a collisional cascade is rapidly set up in the system and the same physics applies

Optical properties

Optical constants can be used to work out the bulk properties of the grains (Q_{abs}, Q_{sca} and Q_{pr}) using **Mie theory** for compact spherical grains, and **geometric optics** and **Rayleigh-Gans** theory in appropriate limits (Laor & Draine 1993)

Astronomical silicate (Draine & Lee 1984)

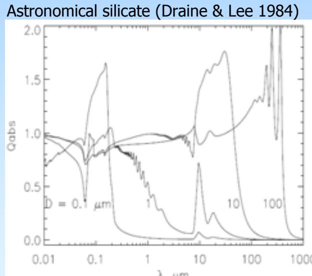

Organic refractory (Li & Greenberg 1997)

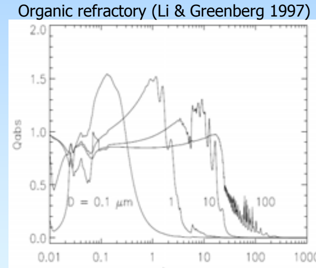

- Emission efficiency $Q_{em}=Q_{abs}$ ~1 for $\lambda<D$ and $\sim(\lambda/D)^n$ for $\lambda>D$ (although there are emission features, e.g., 10 and 20 μm features of silicates from Si-O stretching and O-Si-O bending modes)
- Albedo = $Q_{sca}/(Q_{abs}+Q_{sca})$

Radiation pressure coefficient

Remember $Q_{pr}=Q_{abs}+Q_{sca}[1-\langle\cos(\alpha)\rangle]$ where $\langle\cos(\alpha)\rangle$ is the asymmetry parameter (asymmetry in light scattered in forward/backward direction)

But we're interested in $\beta=F_{rad}/F_{grav}=(1150/\rho D)(L_*/M_*)\langle Q_{pr}\rangle_{T*}$
where $\langle Q_{pr}\rangle_{T*} = \int Q_{pr}F_* d\lambda \; / \; \int F_* d\lambda$ is Q_{pr} averaged over stellar spectrum

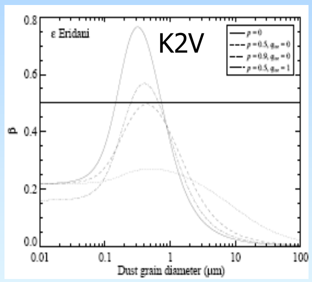

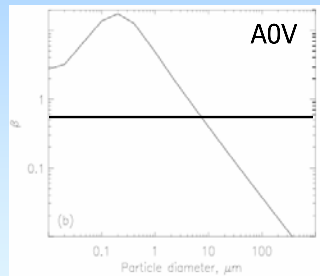

- higher mass stars remove larger grains by radiation pressure (~1μm for K2V and 10μm for A0V)
- porous grains are removed for larger sizes
- turnover at low D means small grains still bound to K and M stars

Equilibrium dust temperature

The equilibrium temperature of a dust grain is determined by the balance between energy absorbed from the star and that re-emited as thermal radiation:

$$[g/(4\pi r^2)] \int Q_{abs}(\lambda,D)\, L_*(\lambda)\, d\lambda = G \int Q_{abs}(\lambda,D)\, B_\nu(\lambda,T(D,r))\, d\lambda$$

where dust temperature is a function of D and r, $g=0.25\pi D^2$, $G=\pi D^2$

Since $\int L_*(\lambda)\, d\lambda = L_*$ and $\int B_\nu(\lambda,T)\, d\lambda = \sigma T^4$, then

$$T(D,r) = [\, \langle Q_{abs}\rangle_{T*} / \langle Q_{abs}\rangle_{T(D,r)} \,]^{0.25}\, T_{bb}$$

where $T_{bb} = 278.3\, L_*^{0.25}\, r^{-0.5}$ and $\langle Q_{abs}\rangle_{T*}$ is average over stellar spectrum

Small particles are hotter than black body because they absorb starlight efficiently, but reemit inefficiently

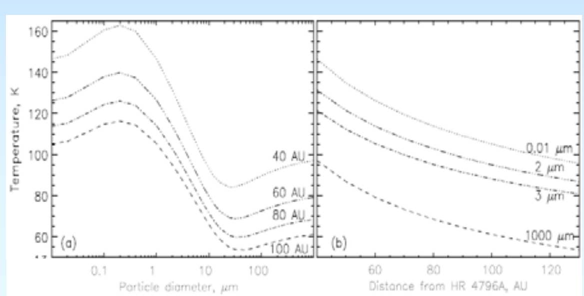

Emission spectrum

The emission from a single grain is given by

$F_\nu(\lambda,D,r) = Q_{abs}(\lambda,D)\, B_\nu(\lambda,T(D,r))\, \Omega(D)$

where $\Omega = 0.25\pi D^2/d^2$ is the solid angle subtended by the particle at the Earth

If the disk is axisymmetric then define the distribution of cross-sectional area such that $\sigma(D,r)dDdr$ is the area in the range D to D+dD and r to r+dr and so $\int\int\sigma(D,r)dDdr = \sigma_{tot}$

Thus the total flux in Jy from the disk is

$$F_\nu = 2.35\text{x}10^{-11} \int_{r_{min}}^{r_{max}}\int_{D_{min}}^{D_{max}} Q_{abs}(\lambda,D)\, B_\nu(\lambda,T(D,r))\, \sigma(D,r)\, d^{-2}\, dD\, dr$$

where area is in AU^2 and distance d is in pc

This equation can be simplified by setting $\sigma(D,r)=\sigma(D)\sigma(r)$ or just $=\sigma(D)$

Even more simply the grains can be assumed to be black bodies $Q_{abs}=1$ at the same distance giving $\mathbf{F_\nu = 2.35x10^{-11}\, B_\nu(\lambda,T_{bb})\, \sigma_{tot}\, d^{-2}}$

Modelling images

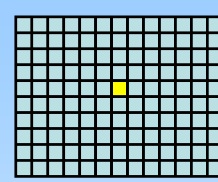

An image is made up of many pixels, each of which has a different line-of-sight through the disk

The surface brightness of emission in each pixel in Jy/sr is worked out using a line-of-sight integrator:

$$F_\nu/\Omega_{obs}=2.35\text{x}10^{-11}\int_{R_{min}}^{R_{max}}\int_{D_{min}}^{D_{max}} Q_{abs}(\lambda,D)B_\nu(\lambda,T(D,r))\sigma(D,r,\theta,\phi)dDd\mathbf{R}$$

where $\sigma(D,r,\theta,\phi)$ is volume density of cross-sectional area in AU^2/AU^3 per diameter, and **R** is the line of sight vector

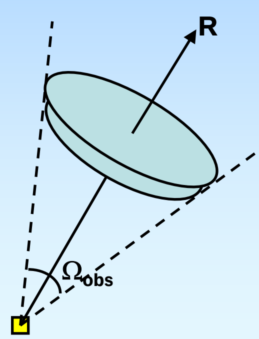

This equation can be simplified by setting

$\sigma(D,r,\theta,\phi)=\sigma(D)\sigma(r,\theta,\phi)$

$F_\nu/\Omega_{obs} = P(\lambda,r)\, \sigma(r,\theta,\phi)\, d\mathbf{R}$

$P(\lambda,r)=2.35\text{x}10^{-11}\int_{D_{min}}^{D_{max}} Q_{abs}(\lambda,D)B_\nu(\lambda,T(D,r))[\sigma(D)/\sigma_{tot}]dD$

where $\sigma(r,\theta,\phi)$ depends on dynamics, and $P(\lambda,r)$ depends on composition/size distribution

Modelling structure

A model for the spatial distribution of material, $\sigma(r,\theta,\phi)$, can be derived from 2 body dynamics and assuming distributions of orbital elements.

For example, in 2D:

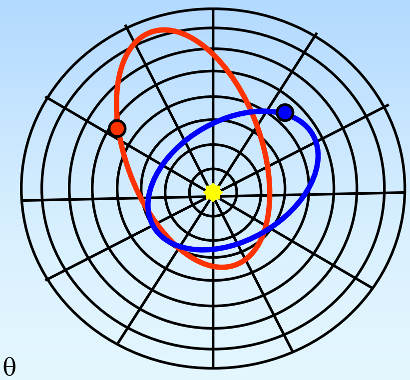

(1) Make a grid in r and θ
(2) Choose N particles on orbits with
- Semimajor axis, a
  e.g., between a_1 and a_2
- Eccentricity, e
  e.g., between 0 and e_{max}
- Pericentre orientation, ϖ
  e.g., between 0^0 and 360^0
- Mean longitude, λ
  e.g., between 0^0 and 360^0

(3) Convert particle location into r and θ
(4) Add up number of particles in each grid cell

Real disk images

The line-of-sight integrator will give a perfect image of the disk, the one that arrives at the Earth's atmosphere

The image is blurred by the point spread function of the telescope
• ideally there will be a psf image to convolve the perfect image with
• if not, can assume Gaussian smoothing with FWHM=λ/Diameter telescope
• this is what you compare to the observation

The images are noisy
• often assume each pixel has additional uncertainty defined by gaussian statistics with given 1σ
• **Monte-Carlo:** to ascertain effect on image, create many noisy model images (each with random noise component) and see how diagnostics of model are affected

Application to Fomalhaut images

The disk modelling process is evident through the example of the Fomalhaut disk (Holland et al. 2003; Wyatt & Dent 2002):

450μm observation | model | residuals

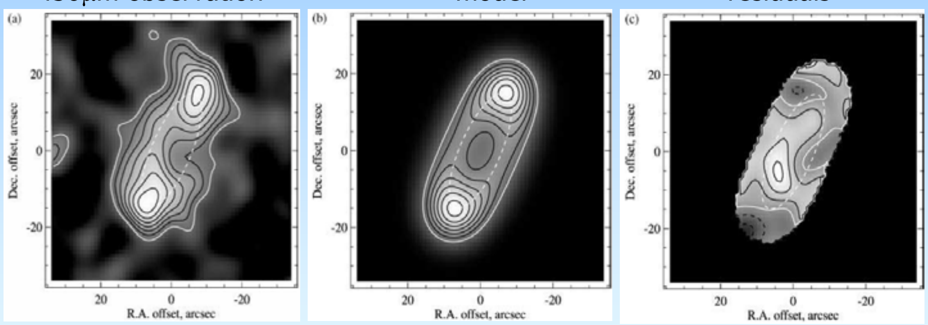

- The observation has three observables: mean peak brightness of the lobes, mean radial offset, mean vertical half maximum width
- The model had three free parameters: total area, radius, and inclination (although slightly more information on radial and vertical structure)

Fomalhaut SED

Once the radial distribution was constrained using the image, the full SED could be used to constrain the size distribution

model changing q | model changing composition

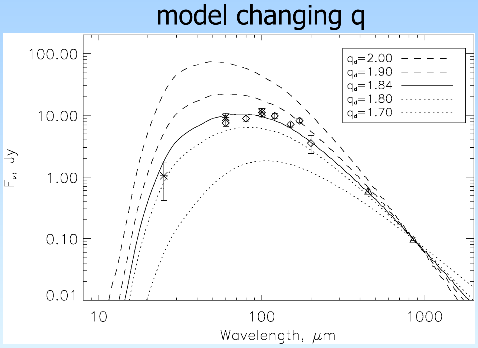

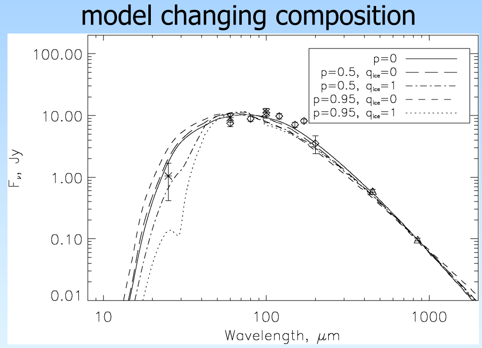

The slope of the size distribution could be well constrained as different dust sizes (at the same distance) have different temperatures, but the composition could not

Extended dust distributions

The extended structure of AU Mic can be explained by dust created in a narrow belt at ~40AU (Augereau & Beust 2006; Strubbe & Chiang 2006)

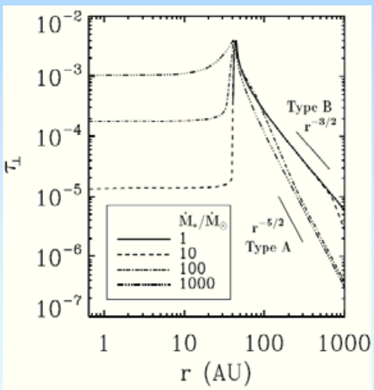

Short wavelengths probe smallest grains and so are dominated by dust on orbits affected by pressure and drag forces

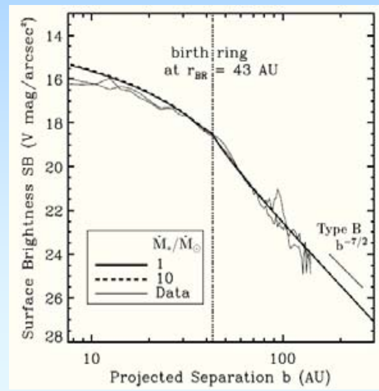

β Pictoris dust distribution can be explained in the same way (Augereau et al. 2001)

Planetary perturbations

Planetesimal belt theory provides a solid model with which to interpret disk structure, because it explains

- **ring structure**
- **extended dust distributions**
- **emission spectrum**
- **dust mass evolution**

Study of the solar system shows that the most important perturbation to the structure and evolution of a debris disk is the formation of massive planets within the disks. Here I will show the effect of planetary perturbations, and how they explain:

- **spiral structure**
- **offsets and brightness asymmetries**
- **clumps**

Observed debris disk asymmetries

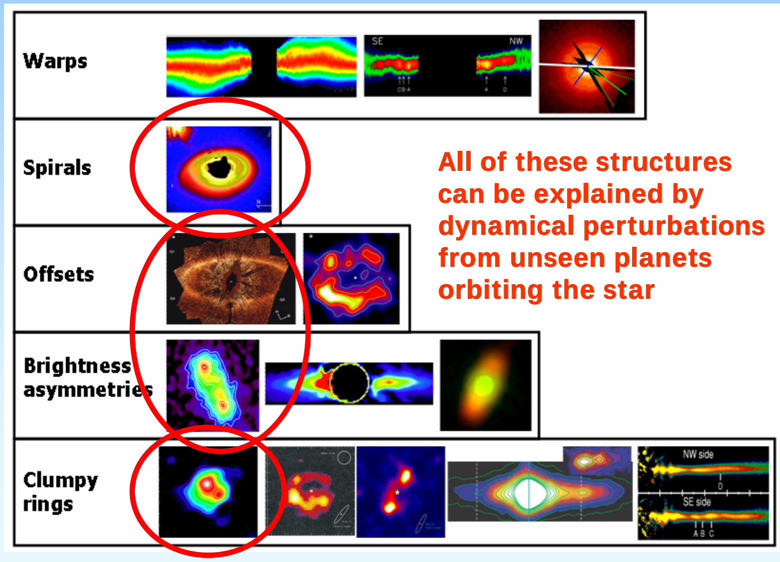

All of these structures can be explained by dynamical perturbations from unseen planets orbiting the star

Gravity!

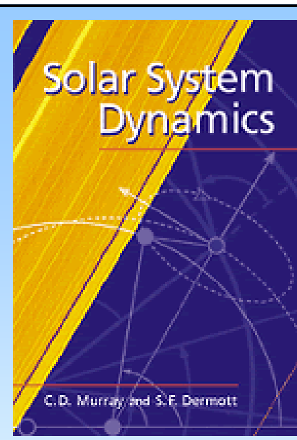

Actually it is exactly this set of features which are predicted from planetary system dynamics

Planetary perturbations

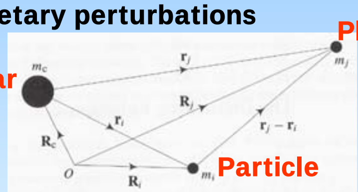

Equation of motion for M_i is: $d^2\mathbf{r}_i/dt^2 = \nabla_i(U_i + \mathcal{R}_i)$
where $U_i = G(M_c+M_i)/r_i$ is the 2 body potential
and $\mathcal{R}_i = GM_j/|\mathbf{r}_j-\mathbf{r}_i| - GM_j\mathbf{r}_i.\mathbf{r}_j/r_j^3$ is the disturbing function

The disturbing function can be expanded in terms of standard orbital elements to an infinite series:

$$\mathcal{R}_i = \mu_j \sum S(a_i,a_j,e_i,e_j,I_i,I_j)\cos(j_1\lambda_i+j_2\lambda_j+j_3\varpi_i+j_4\varpi_j+j_5\Omega_i+j_6\Omega_j)$$

Different types of perturbations

Luckily for most problems we can take just one or two terms from the disturbing function using the **averaging principle** which states that most terms average to zero over a few orbital periods and so can be ignored by using the averaged disturbing function $\langle \mathcal{R} \rangle$

only time dependence, $\lambda = n(t-\tau)$

$$\mathcal{R}_i = \mu_j \sum S(a_i, a_j, e_i, e_j, I_i, I_j)\cos(j_1\lambda_i + j_2\lambda_j + j_3\varpi_i + j_4\varpi_j + j_5\Omega_i + j_6\Omega_j)$$

Terms in the disturbing function can be divided into three types:

- **Secular**
  Terms that don't involve λ_i or λ_j which are slowly varying
- **Resonant**
  Terms that involve angles $\phi = j_1\lambda_i + j_2\lambda_j + j_3\varpi_i + j_4\varpi_j + j_5\Omega_i + j_6\Omega_j$
  where $j_1 n_i + j_2 n_j = 0$, since these too are slowly varying.
- **Short-period**
  All other terms, average out

Lagrange's planetary equations

The disturbing function can be used to determine the orbital variations of the perturbed body due to the perturbing potential using Lagrange's planetary equations:

$da/dt = (2/na)\partial\mathcal{R}/\partial\varepsilon$
$de/dt = -(1-e^2)^{0.5}(na^2e)^{-1}(1-(1-e^2)^{0.5})\partial\mathcal{R}/\partial\varepsilon - (1-e^2)^{0.5}(na^2e)^{-1}\partial\mathcal{R}/\partial\varpi$
$d\Omega/dt = [na^2(1-e^2)\sin(I)]^{-1}\partial\mathcal{R}/\partial I$
$d\varpi/dt = (1-e^2)^{0.5}(na^2e)^{-1}\partial\mathcal{R}/\partial e + \tan(I/2)(na^2(1-e^2))^{-1}\partial\mathcal{R}/\partial I$
$dI/dt = -\tan(I/2)(na^2(1-e^2)^{0.5})^{-1}(\partial\mathcal{R}/\partial\varepsilon + \partial\mathcal{R}/\partial\varpi) - (na^2(1-e^2)^{0.5}\sin(I))^{-1}\partial\mathcal{R}/\partial\Omega$
$d\varepsilon/dt = -2(na)^{-1}\partial\mathcal{R}/\partial a + (1-e^2)^{0.5}(1-(1-e^2)^{0.5})(na^2e)^{-1}\partial\mathcal{R}/\partial e +$
$\quad \tan(I/2)(na^2(1-e^2))^{-1}\,\partial\mathcal{R}/\partial I$

where $\varepsilon = \lambda - nt = \varpi - n\tau$

Tip: as with all equations, these can be simplified by taking terms to first order in e and I

Secular perturbations between planets

- To second order the secular terms of the disturbing function for the j^{th} planet in a system with N_{pl} planets are given by:

$$\mathcal{R}_j = n_j a_j^2[0.5A_{jj}(e_j^2-I_j^2) + \Sigma^{Npl}_{i=1,\, i\neq j} A_{ij}e_ie_j\cos(\varpi_i-\varpi_j) + B_{ij}I_iI_j\cos(\Omega_i-\Omega_j)]$$

where $A_{jj} = 0.25n_j\, \Sigma^{Npl}_{i=1,i\neq j}\, (M_i/M_*)\alpha_{ji}\underline{\alpha}_{ji}b^1_{3/2}(\alpha_{jj})$

$A_{ji} = -0.25n_j(M_i/M_*)\, \alpha_{ji}\underline{\alpha}_{ji}b^2_{3/2}(\alpha_{ji})$

$B_{ji} = 0.25n_j(M_i/M_*)\, \alpha_{ji}\underline{\alpha}_{ji}b^1_{3/2}(\alpha_{ji})$

α_{ji} and $\underline{\alpha}_{ji}$ are functions of a_i/a_j and $b^s_{3/2}(\alpha_{ji})$ are Laplace coefficients

- Converting to a system with $z_j = e_j \exp(i\varpi_j)$ and $y_j = I_j \exp(i\Omega_j)$ and combining the planet variables into vectors $\mathbf{z} = [z_1,z_2,\ldots,z_{Npl}]^T$ and for $\mathbf{y}$ gives for Lagrange's planetary equations

$da_j/dt = 0$, $d\mathbf{z}/dt = iA\mathbf{z}$, $d\mathbf{y}/dt = B\mathbf{y}$, where A,B are matrices of A_{ji},B_{ji}

- This can be solved to give:

$z_j = \Sigma^{Npl}_{k=1}\, e_{jk} \exp(ig_k+i\beta_k)$ and $y_j = \Sigma^{Npl}_{k=1}\, I_{jk} \exp(if_kt+i\gamma_k)$

where g_k and f_k are the eigenfrequencies of A and B and β_k γ_k are the constants

Secular perturbations of eccentric planet on planetesimal orbit

Taking terms to second order in e and I, Lagrange's planetary equations are:

$$dz/dt = iAz + i\Sigma^{Npl}_{j=1} A_jz_j$$

where $z=e^*\exp[i\varpi]$
with a similar equation for $y=I^*\exp[i\Omega]$.

$$z = z_f + z_p$$
$$= \sum^{Npl}_{k=1}\Big[\Sigma^{Npl}_{j=1}\big[A_je_{jk}\big]/(g_k-A)\exp(ig_kt+i\beta_k)\Big]$$
$$+\, e_p \exp(iAt+i\beta_0)$$

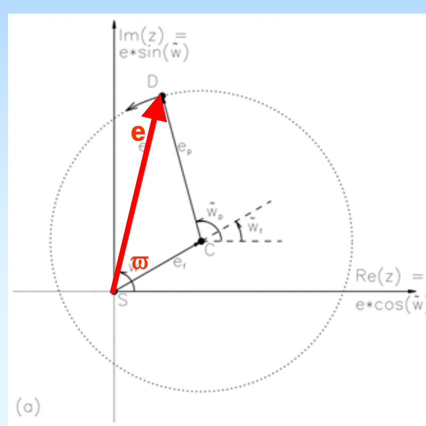

Meaning the orbital elements of planetesimals precess around circles centred on forced elements imposed by planetary system

Murray & Dermott (1999)

Post planet formation evolution

Consider impact of sudden introduction of planet on eccentric orbit on extended planetesimal belt for which eccentricity vectors start at origin

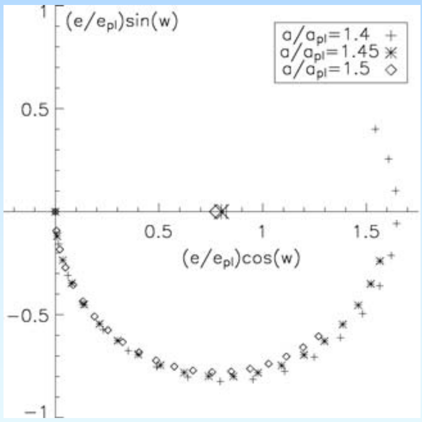

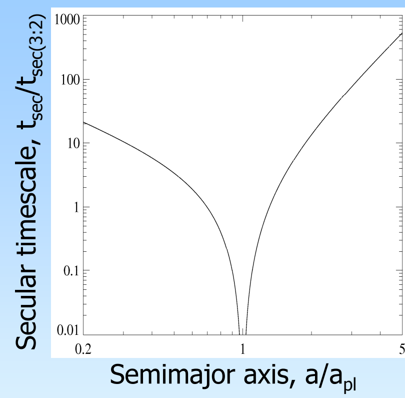

Precession rates are slower for planetesimals further from planet which means dynamical structure evolves with time

$$t_{sec(3:2)} = 0.651 t_{pl}/(M_{pl}/M_{star})$$

Wyatt (2005)

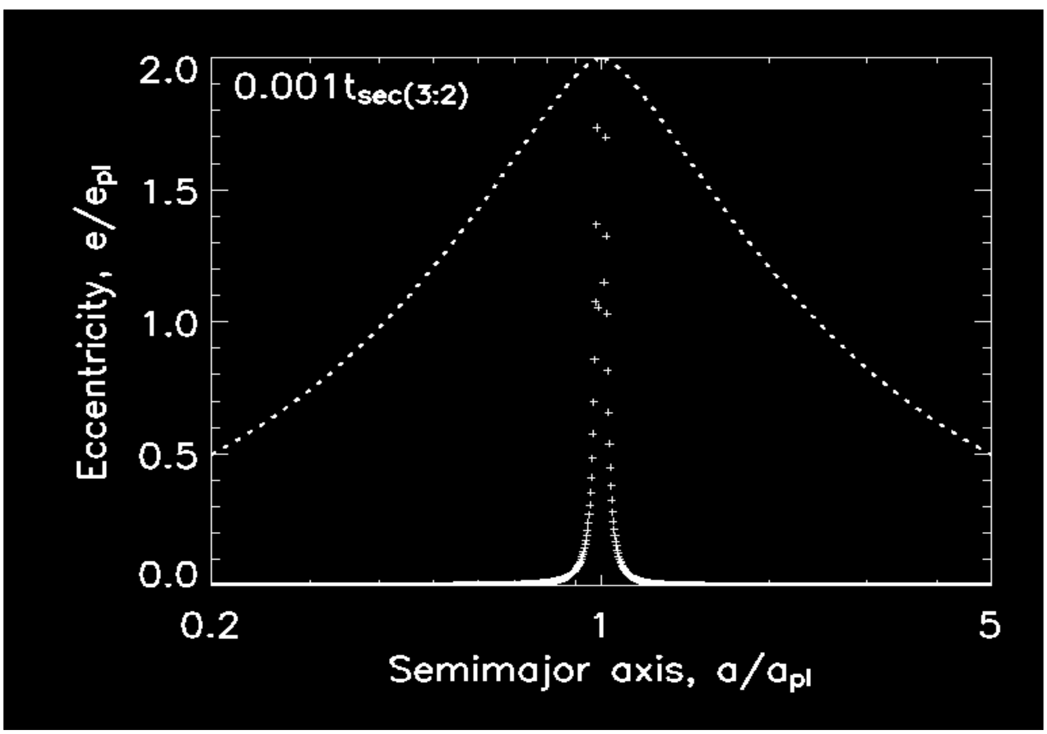

Converting dynamical structure to spatial distribution

(1) Make a grid in r and θ

(2) Choose N particles on orbits with
- Semimajor axis, a
  between a_1 and a_2
- Eccentricity, e
  where e depends on a and t
- Pericentre orientation, ϖ
  where ϖ depends on a and t
- Mean longitude, λ
  between 0^0 and 360^0

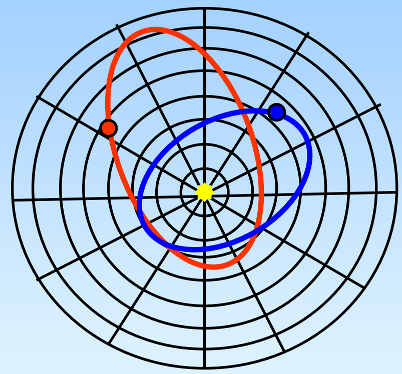

(3) Convert particle location into r and θ

(4) Add up number of particles in each grid cell

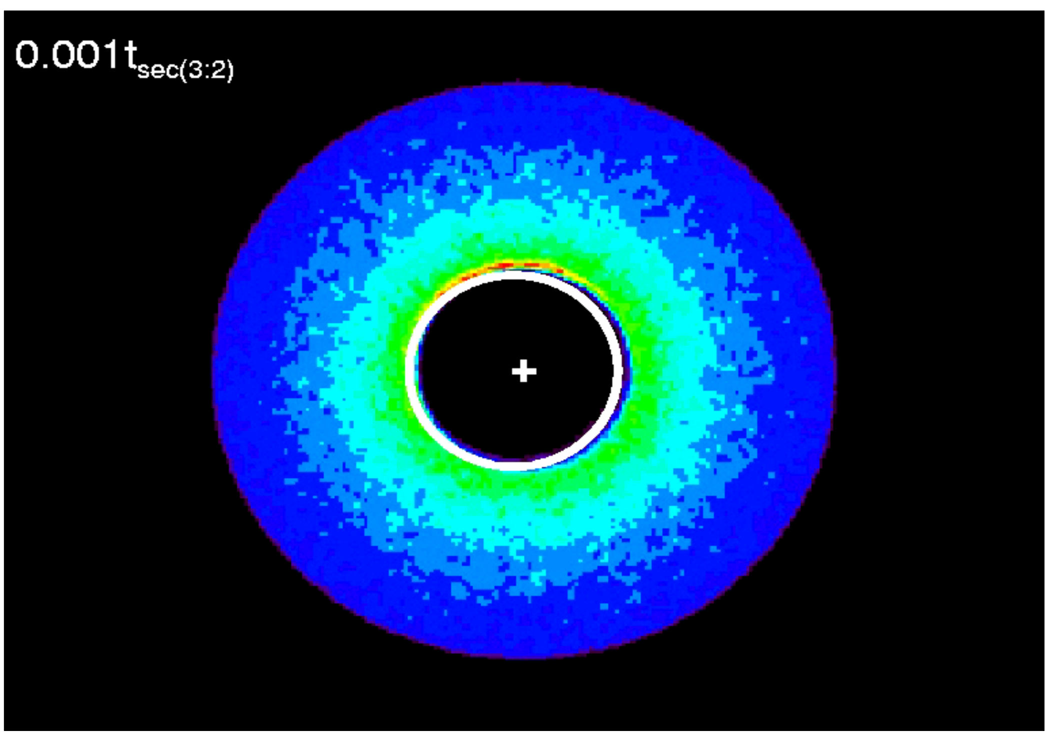

Spiral Structure in the HD141569 Disk

- HD141569A is a **5 Myr**-old **B9.5V** star at **99 pc**
- Dense rings at 200 and 325 AU with tightly wound spiral structure (Clampin et al. 2003)

Observation

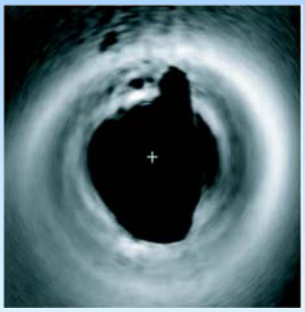

Wyatt (2005)

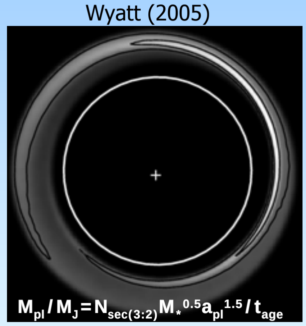

Augereau & Papaloizou (2004)

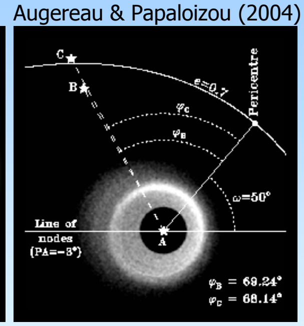

- Spiral structure at 325 AU can be explained by:
  - $0.2M_{Jupiter}$ planet at 250AU with e=0.05 (Wyatt 2005)
  - binary companion M stars at 1200AU (Augereau & Papaloizou 2004)
- Spiral structure at 200 AU implies planet at 150 AU
- Same structure seen in Saturn's rings (Charnoz et al. 2005) but for different reason…

Perturbations at late times in narrow ring

Consider planetesimals with same proper eccentricities e_p at semimajor axis a

After many precession periods, orbital elements distributed evenly around circle centred on z_f

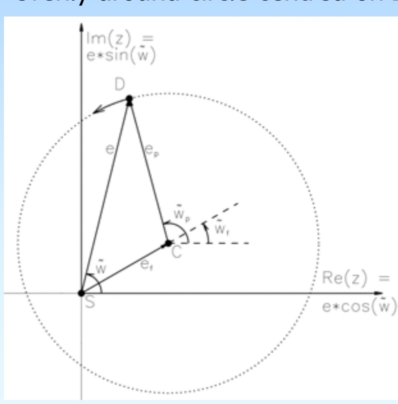

This translates into material in a uniform torus with centre of symmetry offset from star by ae_f in direction of forced apocentre

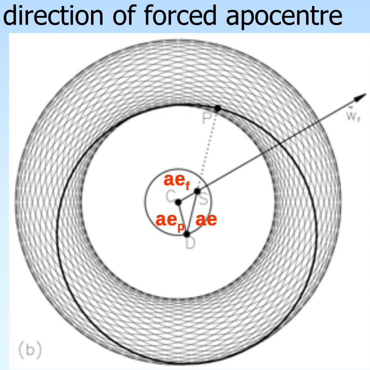

Pericentre glow in HR4796

Phenomenon predicted based on observations of the dust ring around HR4796 (A0V , 10Myr) (Wyatt et al. 1999)

NE lobe is 5% brighter than SW lobe

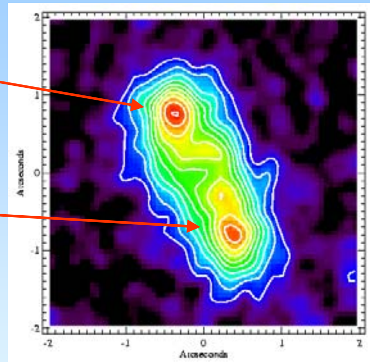

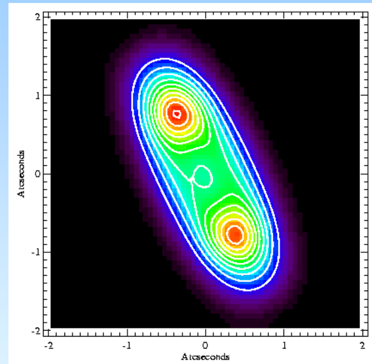

Model fitting like Fomalhaut with:
- four observables (lobe distance, brightness, vertical distribution, brightness asymmetry)
- five free parameters (radius, total area, inclination, forced eccentricity, pericentre orientation)

Interpretation of HR4796

The forced eccentricity causes the forced pericentre side to be closer to the star and so hotter and brighter than the opposite side

The forced eccentricity required to give 5% asymmetry is dependent on the orientation of the forced pericentre to the line-of-sight

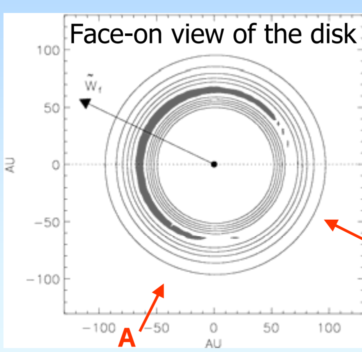

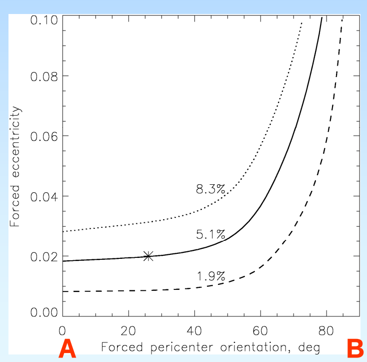

The 5% asymmetry is likely caused by $e_f \sim 0.02$

Origin of forced eccentricity

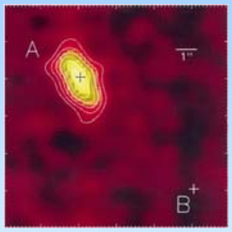

There is an M star binary companion at 517AU the orbit of which is unknown, but an eccentricity of ~0.13 could have imposed this offset

But then again, so could a planet with e_{pl}=0.02

Most likely both binary and planet are perturbing the disk leading to a complex forced eccentricity distribution

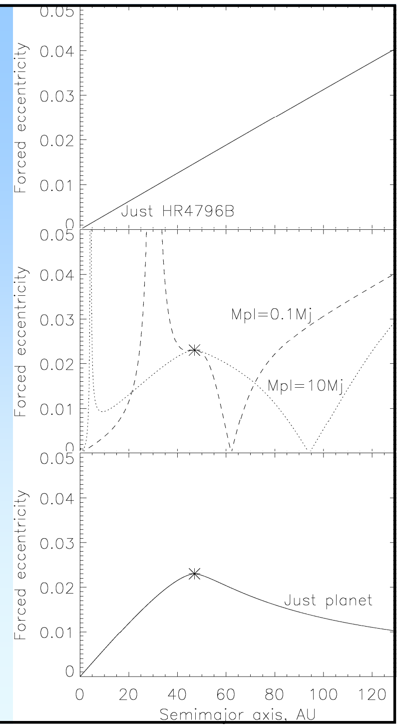

Offset in Fomalhaut

While the offest in HR4796 remains unconfirmed, it has been confirmed in HST imaging of Fomalhaut (Kalas et al. 2005)

Image shows a ~133AU radius ring with a centre of symmetry offset by 15 AU from the star, implying a forced eccentricity of ~0.1

Fomalhaut has an M star binary companion at 2° (50,000AU, 0.3pc), which could perturb the ring, but not that much (a_B>25,000AU so $a_{ring}/a_B<5\times10^{-3}$ and $e_{ring}<5\times10^{-3}$)

However, the sharp inner edge implies presence of another perturber (Quillen 2006)

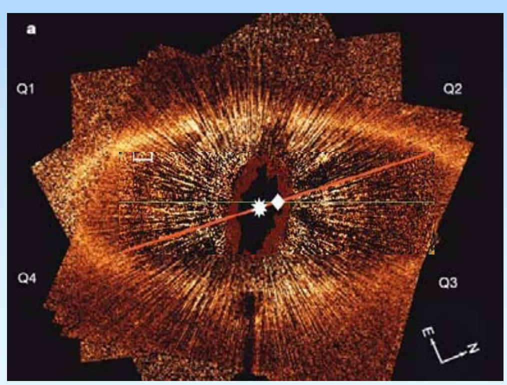

Geometry of resonance

- A resonance is a location where a planetesimal orbits the star **p** times for every **p+q** planet orbits, which occurs at $\mathbf{a}_{\mathbf{res}}=a_{pl}$ [$(p+q)/p$]$^{2/3}$

- Resonances are special because of the periodic nature of the orbits and the way that planet and planetesimal have encounters

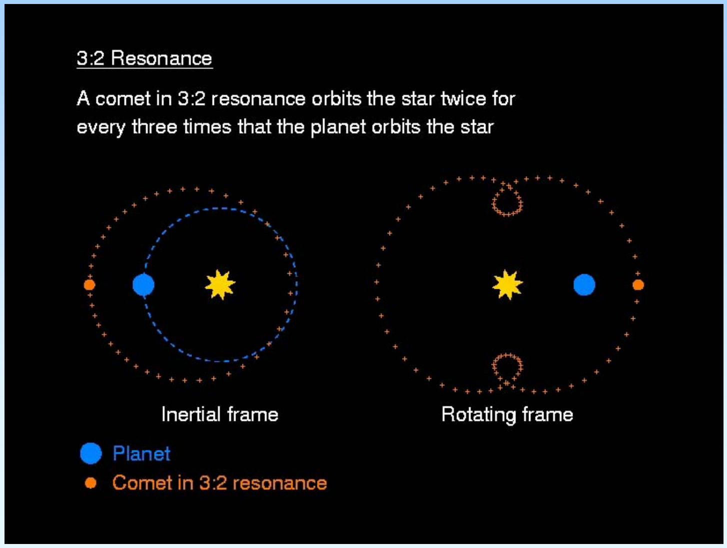

Geometry of resonance

- Orientation of the loopy pattern is defined by the resonant angle, e.g.
  $$\phi = (p+q)\lambda - p\lambda_{pl} - q\varpi$$
  $$= p[\varpi - \lambda_{pl}(t_{peri})]$$
  which is the appropriate term in the disturbing function

- ϕ librates about 180^o for all but the n:1 resonance for which this is function of eccentricity (=**asymmetric libration**)

Each resonance has its own geometry

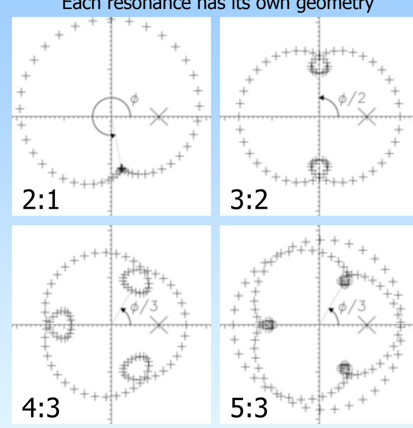

Capture by migrating planet

Planetesimals can become captured into the resonances of a migrating planet

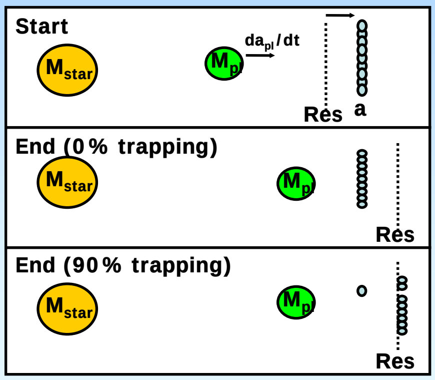

Numerical integrations of star, migrating planet, 200 planetesimals giving capture probabilities for 3:2 resonance:

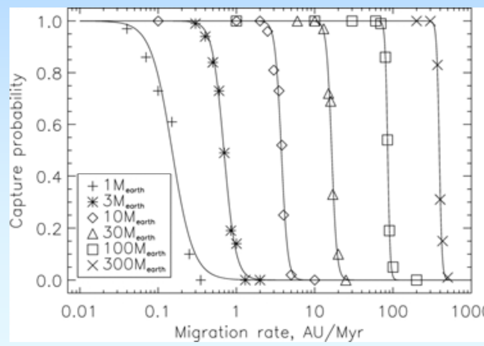

Capture probability dependencies

The runs were performed changing planet mass, planetesimal semimajor axis and stellar mass

Probability of capture into a resonance as it passes is a function only of (Wyatt 2003)

$\mu = M_{pl}/M_*$

$\theta = (da_{pl}/dt)(a/M_*)^{0.5}$

$P = [1+(0.37\mu^{-1.37}\theta)^{5.4\mu^{\wedge}0.38}]^{-1}$

Following capture the eccentricity of a planetesimal is pumped up according to the relation:

$e^2 = e_0^2 + [q/(p+q)]\ln(a/a_0)$

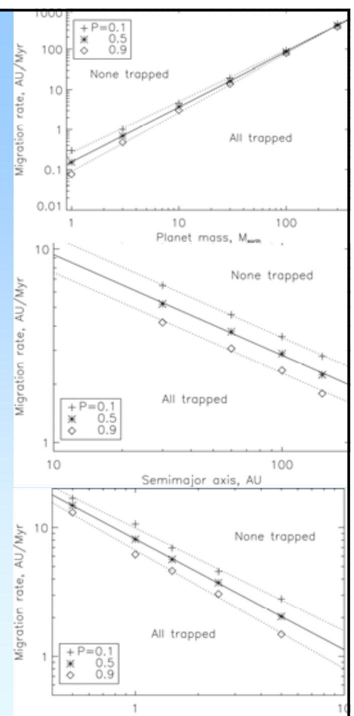

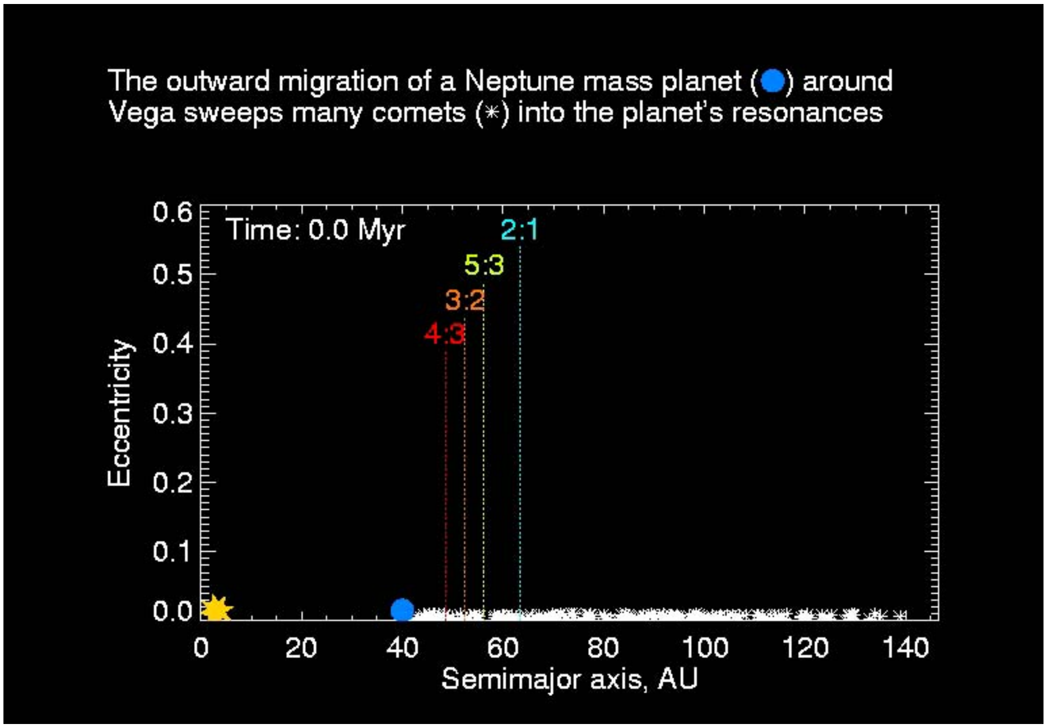

Resonant spatial distribution

The location of planetesimals in the grid depends on their semimajor axis, a, eccentricity, e, and resonant angle, ϕ, with random longitude, λ:

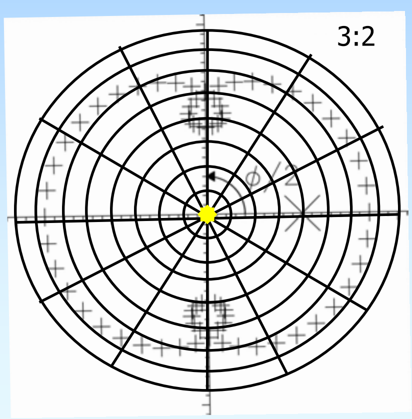

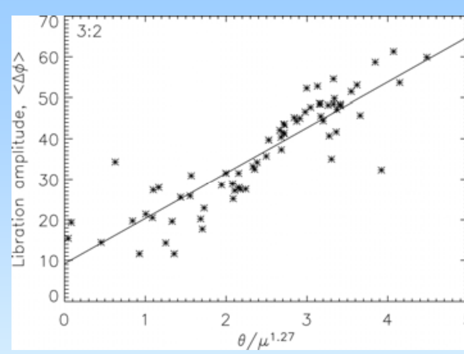

Since the resonant angle librates

$\phi = \phi_m + \Delta\phi \sin(2\pi t/t_\phi)$

To determine the spatial distribution we need to know:

$\phi_{m3:2} = 180^o + 7.5(\theta/\mu) - 0.23(\theta/\mu)^2$

$\Delta\phi_{3:2} = 9.2^o + 11.2(\theta/\mu^{1.27})$

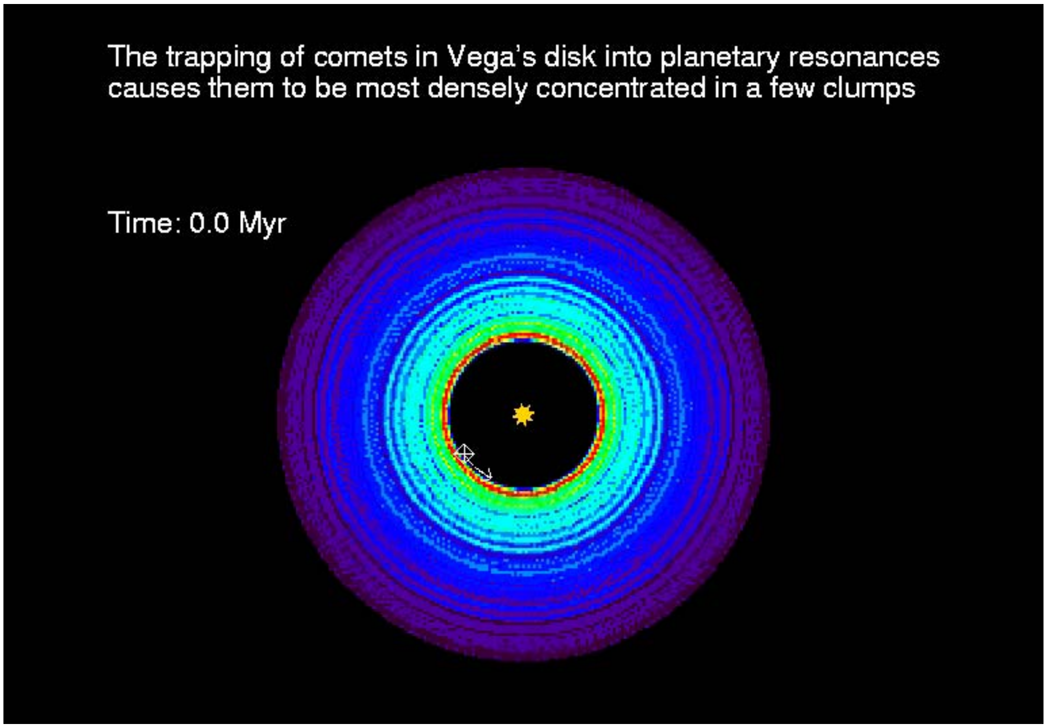

Constraints on Vega's planetary system

Observation

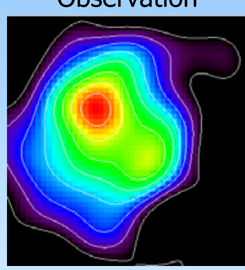

Model

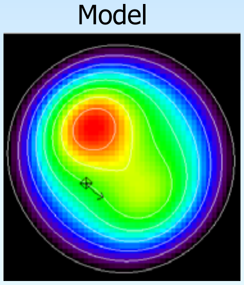

The two clumps of asymmetric brightness in sub-mm images of Vega's debris disk (Holland et al. 1998) can be explained if planet mass and migration rate fall in a certain region of parameter space ( ) (Wyatt 2003)

Planet migration rate

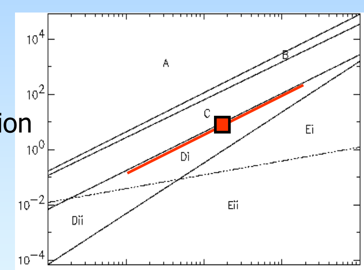

Planet mass

At $1M_{neptune}$ and 56Myr migration timescale ( ), implies Vega system formed and evolved like solar system

Dynamics of small bound grains

- Radiation pressure alters orbital period of dust and so its relation to resonance; $\Delta a = a_d - a_{rd} = a_r\beta(4/3 \pm 2e)$
- Small grains have higher libration widths than planetesimals
- Particles smaller than **$200\mu m\ (L_\star / M_\star)\mu^{-0.5}$** fall out of resonance

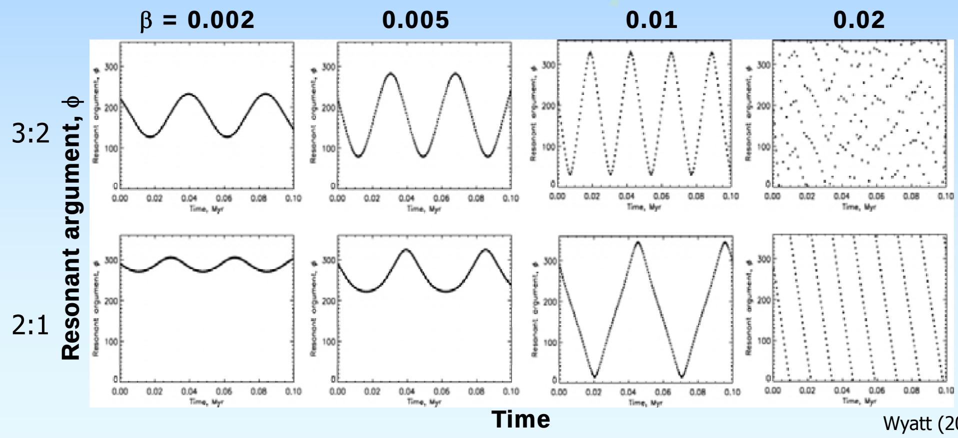

Wyatt (2006)

Distribution of small bound grains

- Large particles have the same clumpy distribution as the parent planetesimals
- The increased libration width of moderate sized grains smears out clumpy structure
- The smallest bound grains have an axisymmetric distribution

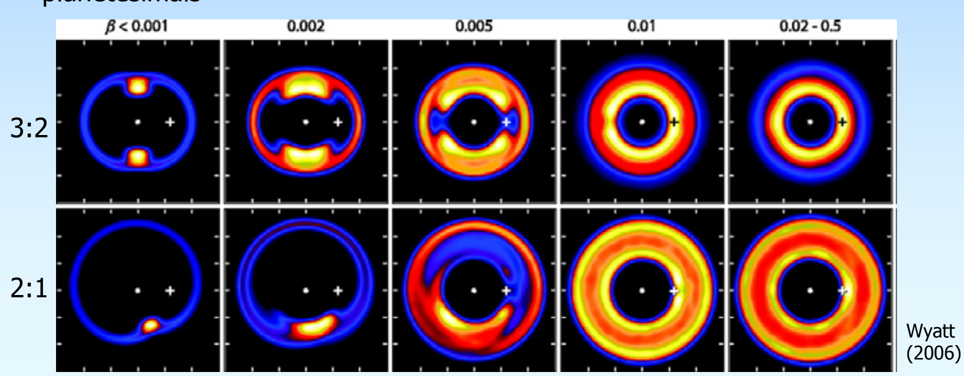

Wyatt (2006)

Dynamics of small unbound grains

- Radiation pressure puts small (β>0.5) grains on hyperbolic trajectories
- The collision rate (R_{col}) of resonant planetesimals is higher in the clumps
- In model, work out R_{col} by looking at number of planetesimals within 4AU and average relative velocity

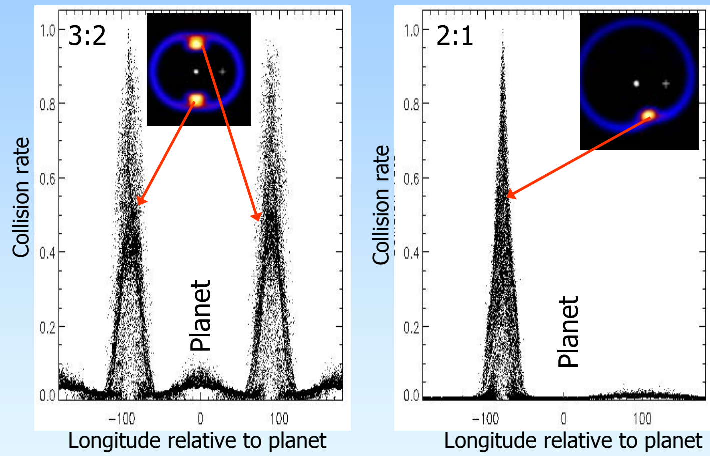

Blow-out grains exhibit spiral structure if created from resonant planetesimals

Particle populations in a resonant disk

Grain size population		**Spatial distribution**
Large	I	Same clumpy distribution as planetesimals
Medium	II	Axisymmetric distribution
Small	III	$\tau \propto r^{-1}$ distribution
	IIIa	Spiral structure emanating from resonant clumps
	IIIb	Axisymmetric distribution

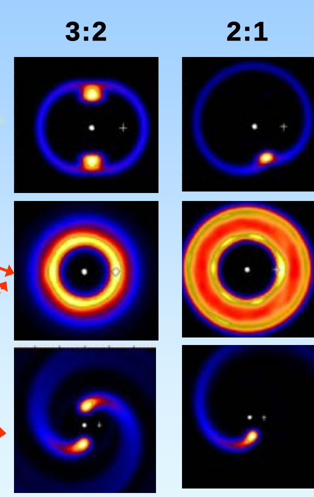

What does this mean for Vega?

SED modelling used to determine the size distribution…

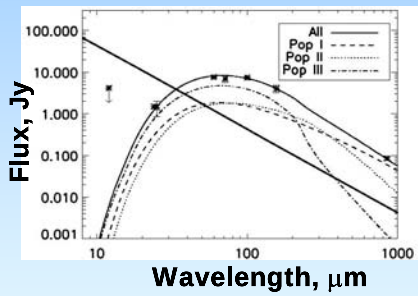

… then used to assess contribution of grain sizes to observations:

- Sub-mm samples pop I
- Mid- and far-IR sample pop III

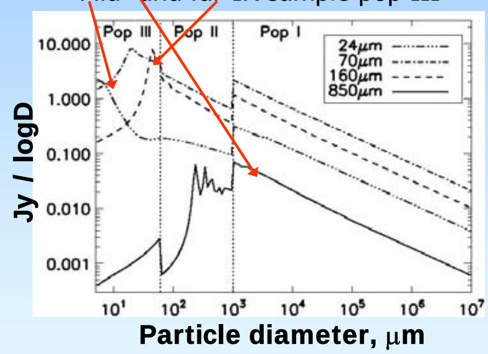

Observations in different wavebands sample different grain sizes and so populations, thus multi-wavelength images should show different structures and can be used to test models

Wyatt (2006)

Comparison with observations

Mid- to far-IR images should exhibit spiral structure emanating from clumps

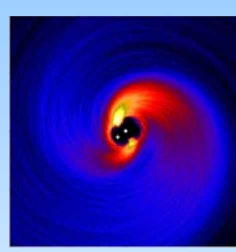

Meanwhile 350μm imaging shows evidence for 3 clump structure (Marsh et al. 2006)

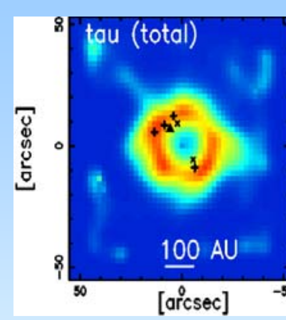

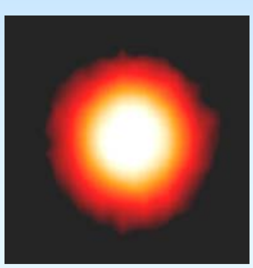

Not detected at present, but resolution of published Spitzer observations may not have had sufficient resolution to detect this (Su et al. 2005)

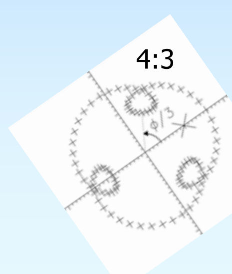

Possible evidence for a different size distribution of material in 4:3 resonance?

Resonant structure follows the planet

- The model can be tested by multi-epoch imaging of the clumpy sub-mm structure, since resonant structures orbit with the planet

- Decade timescales for confirmation, and there is already a 2σ detection of rotation in disk of ε Eri (Poulton et al. 2006)

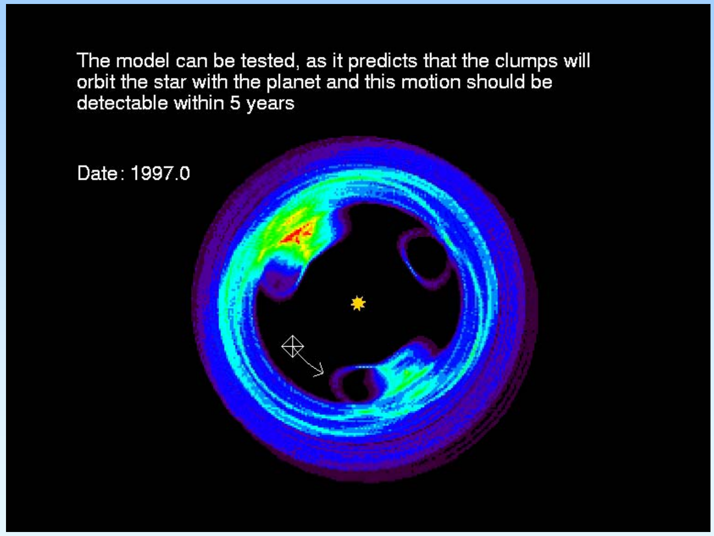

Dust migration into planetary resonances

Resonances can also be filled by inward migration of dust by P-R drag, since resonant forces can halt the migration

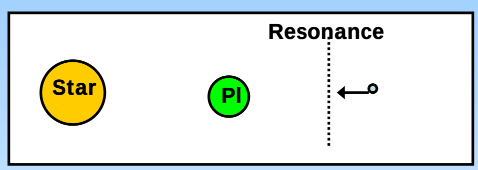

For example dust created in the asteroid belt passes the Earth's resonances and much of it is trapped temporarily (~10,000yrs)

Trapping timescale is of order t_{pr} meaning ring forms along Earth's orbit

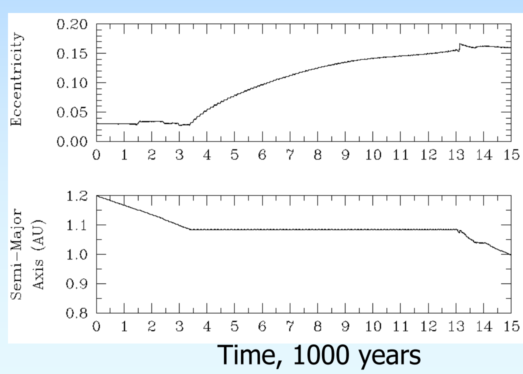

Structures of resonant rings

The structure expected when dust migrates into planetary resonances depends on the planet's mass and eccentricity
(Kuchner & Holman 2003)

However, this ignores that P-R drag is not important in detectable debris disks

low M_{pl} | high M_{pl}

low e_{pl}

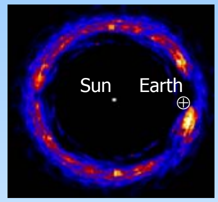

Dermott et al. (1994)

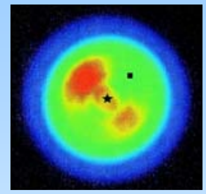

Ozernoy et al. (2000)

high e_{pl}

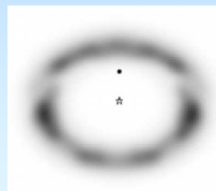

Quillen & Thorndike (2002)

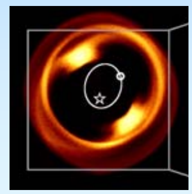

Wilner et al. (2002)

Why P-R drag is insignificant

Remember that the surface density of a disk evolving due to collisions and P-R drag is only determined by the parameter

$\eta_0 = 5000\tau_{eff}(r_0)[r_0/M_*]^{0.5}/\beta$

This is an observable parameter, since r_0 can be estimated from dust temperature, $\beta<0.5$, and

$\tau_{eff} \approx 6.8\text{x}10^9\ d^2F_\nu/[rdrB_\nu(T)]$

Wyatt (2005)

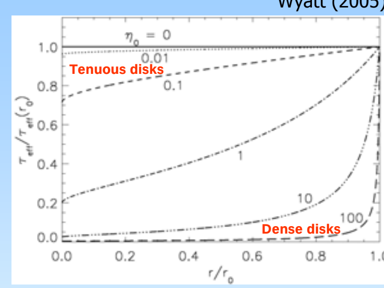

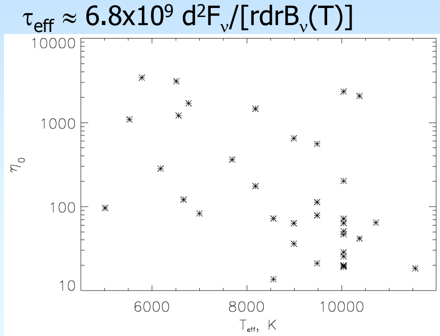

For the 38 disks detected at more than one wavelength (for which T can be estimated) P-R drag is insignificant

When P-R drag becomes important

The reason is that detectable disks have to be dense to have a flux that exceeds that of the photosphere

This is only possible for η_0>1 for distant belts around high mass stars detected at long wavelengths…

… although low η_0 disks can be detected if they are resolved (ALMA/ JWST/ TPF/ DARWIN)…

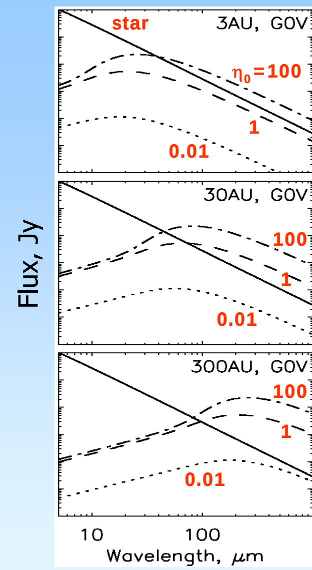

… at which point we may be able to detect the resonant rings of Earth-like planets more readily than the planets themselves!

Conclusions

Modelling debris disks can provide information about unseen planetary systems

These currently occupy the uncharted Saturn, Uranus, Neptune region of parameter space

Future observations will probe the Earth, Venus regions